Cranfield

College of Aeronautics Report No. 8906
May 1989

A summary of the scale model wind tunnel tests on the TRRL spray dispersion articulated tanker vehicle

Kevin P Garry

College of Aeronautics
Department of Aerodynamics
Cranfield Institute of Technology
Cranfield. Bedford MK43 0AL. England

Cranfield

College of Aeronautics Report No. 8906
May 1989

A summary of the scale model wind tunnel tests on the TRRL spray dispersion articulated tanker vehicle

Kevin P Garry

College of Aeronautics
Department of Aerodynamics
Cranfield Institute of Technology
Cranfield. Bedford MK43 0AL. England

ISBN 1 871315 04 2

£8.00

SUMMARY

The aerodynamic characteristics of articulated tanker vehicles are thought to be sufficiently different from those of conventional box container vehicles to warrant investigation. The results from a programme of experimental studies using scale wind tunnel models are presented, the primary aim of which is to investigate the effectiveness of established aerodynamic drag reducing and spray suppression devices when used on articulated tankers.

Analysis suggests that the tanker flowfield is different from that expected for box container vehicles, particularly in the region of the tractor-trailer gap. Consequently, devices intended to control the flow in this region, and designed specifically for box containers, are not as effective on tanker vehicles. In particular, cab roof mounted fairings and tractor-trailer gap seals are seen to require modification to achieve comparable reductions in drag.

Attempts to simulate the dispersion of water spray generated by the tyres in wet weather using paraffin smoke are assessed. The technique is thought to over simplify the complex nature of water spray dispersion but is considered a useful first step prior to full scale trials.

CONTENTS

1. INTRODUCTION

Recent interest in the aerodynamic characteristics of commercial vehicles has concentrated on the improvements in fuel efficiency that are possible due to reductions in aerodynamic drag. An associated factor, concerning the flow around this type of vehicle, is the dispersion of water spray in wet weather. It would seem feasible that modifications could be made to conventional vehicle designs that would reduce both drag and spray dispersion.

With this objective, a long term research programme was begun by the Transport and Road Research Laboratory (TRRL) with the aim of quantifying the reductions in aerodynamic drag and water spray dispersion that are possible through the use of specific modifications to a conventional vehicle. The programme involved both wind tunnel tests on scale models at the College of Aeronautics (under contract to TRRL) and full scale trials on the TRRL test track at Crowthorne, Berkshire. The vehicle configuration chosen for the tests was a standard 40 ft articulated box container with an alternative of two tractor units; a Leyland T45 and a DAF 3300. Detailed results from each phase of this programme are given by the author (1), (2) and by Cowperthwaite (3). In simple terms, the results suggest that tractor and trailer side skirts - the devices recognised as being most likely to reduce water spray dispersion - also give a reduction in wind averaged drag coefficient (C_DWAV). The drag reduction was seen to be proportional to the extent of cover offered by the skirts and, within the limits of the test programme, did not appear to be dependent on tractor geometry.

During the programme, and parallel studies associated with the work, it became apparent that within the class of commercial vehicles under consideration, box container trailers, were not necessarily the worst in terms of spray dispersion. Articulated tanker vehicles were seen to produce very high levels of spray. The aerodynamic characteristics of tanker vehicles are known to be very different from those of conventional box containers. Work by the author (4) and others has shown that the aerodynamic forces generated are considerably different and that the flowfield, particularly between the tractor and tanker forebody, can be significantly different to that seen on a conventional box container vehicle.

In view of this, it was considered necessary to extend the initial programme to investigate articulated tanker vehicles, and this report deals specifically with those tests.

2. MAIN OBJECTIVES OF THE PROGRAMME

The tanker programme was aimed, as was the programme for the box container vehicle which preceded it, to correlate the reductions in aerodynamic drag and water spray dispersion that are possible with various modifications to the vehicle. The modifications chosen followed along similar lines to those adopted by Allen et al. (5) in which (a) the flow around the wheel areas is restricted by the use of 'side skirts' and (b) attempts are made to control the flow in the gap between the tractor and trailer with various seals and deflectors. The programme aimed to quantify the changes in aerodynamic forces in the wind tunnel and also to visualise the vehicles' wake in order to make a qualitative assessment of the likely change in spray dispersion. This procedure is to be supplemented by full scale trials on the spray test track at TRRL, but only the scale model wind tunnel tests are considered here.

3. TEST PROCEDURE

3.1 Wind tunnel model

As a result of the initial programme of research with box container vehicles, existing 1/8th scale models of two tractor units were available. These tractors had been chosen because they represent two very different aerodynamic designs; the Leyland T45 is a relatively streamlined cab offering little protection to the trailer from the freestream flow, and the DAF 3300 is a much more bluff shape for which the flow separates at the forward leading edges effectively shrouding the trailer in its wake. In view of (a) practical considerations with possible full scale tests and (b) the need to emphasise the flow around the tanker, it was decided to use the Leyland T45 tractor unit for the articulated tanker programme.

The essential features of tanker trailers are much less easily defined than those of box trailers and consequently the choice of tanker unit much more difficult. It was decided to use a 'hybrid tanker', not modelled on any specific existing design but having the features considered significant to the aerodynamic characteristics of the vehicle, namely:

(1) adjustable incidence (or pitch) of the tanker unit;
(2) streamlined or sharp leading (and trailing) edges to the tank;
(3) ancillary components such as: access hatches, ladders, side crash bars and a trailer stand.

The resulting vehicle, loosely based on a Crane Frauhauf trailer, is shown in figures (1) and (2). Adjustment of the tank incidence was made by inserting simple spacers between the tractor and trailer mounting block, at the approximate location of the 'king pin'. The incidences chosen were intended to reflect the typical range used on current articulated tanker vehicles.

Various 'add-on' flow control devices were available for the test programme as follows:

1. Tractor-trailer gap seals

Both horizontal and vertical gap seals were investigated consisting of rectangular planform thin flat plates mounted normal to the tanker forebody centreline, see figures (5) and (6). In each case 'small' and 'large' seals were used corresponding to (a) the practical maximum forward extension possible to allow the vehicle to articulate, and (b) a seal extending forward by 80% of the available tractor-trailer separation, respectively.

2. Tractor side skirts

Various forms of skirt arrangement were available for the trailer extending from the rear of the tractor wheel arch to the rear of the trailer wheel arch. 'Full trailer skirts' imply that the skirt extends to cover the trailer wheels, while 'partial skirts' leave the wheels open. In each case 'covered' or 'open' styles were used in which the skirt was folded around the wheel arch to form an enclosed region - 'covered', or simply left as a vertical curtain - 'open', see figures (7) and (8). As the above arrangements effectively link the trailer and tractor they represent practical design problems for articulation and therefore an alternative 'shortened partial trailer skirt' was evaluated, see figure (9).

3. Cab roof mounted fairing

The standard cab roof fairing, figure (10), was chosen to represent the commercially available deflector for the Leyland T45. An alternative 'tanker' cab roof fairing was designed to accommodate the type of flow expected around the tanker, see figure (11), which was capable of being extended to form the roof fairing and cab side extension shown in figures (12) and (13).

3.2 Wind tunnel test technique

The experimental programme was carried out in two different wind tunnels using the same scale model.

The aerodynamic force and moment measurements were made in the 2.4 m x 1.8 m (8' x 6') low speed wind tunnel. This is a closed working section, closed return circuit facility with a maximum speed of 60 metres/second. This enabled tests to be carried out at a Reynolds number, based on $(A)^{\frac{1}{2}}$, of $\approx 1.10 \times 10^6$, corresponding to 1/5th of the full scale Reynolds number at 55 mph. In order to increase the accuracy of the aerodynamic lift measurement, the conventional 'ground board plate' test technique used in the wind tunnel was changed to allow the model to be connected to the overhead balance directly through the base of the wheels, see figure (3). Although not an exact representation of ground proximity, this technique was used to enable crosswind angles of up to 20 degrees to be simulated simply by yawing the model relative to the freestream.

Analysis of the vehicles' external flowfield was made in the 2.4 m x 1.2 m boundary layer wind tunnel. This is an open return, closed working section facility which has an 11 metre long parallel sided flow development section, see figure (4). It is therefore possible, with the model mounted on the floor of the flow development section, to analyse the flow in the wake of the vehicle up to four body lengths downstream. The ground plane is of course fixed and therefore not an accurate simulation of the full scale flow. However the size and complexity of the moving ground plane for such an investigation could not be justified. Boundary layer suction control ahead of the model ensures that the influence of the fixed ground plane is kept to a minimum.

A qualitative assessment of the wake flow was made by injecting paraffin smoke into the flow at specified locations on the vehicle and visualising the resulting plume with a light sheet placed normal to the freestream flow direction, downstream. Photographs of the illuminated plume were taken with a long focal length camera positioned on the working section centre line 10 metres downstream of the model base. The photographs formed the basis of the sketches of the spray propagation patterns presented in this report, see figures (42) to (44).

4. TEST PROGRAMME

4.1 Aerodynamic force and moment measurements

A summary of the 36 tanker vehicle configurations tested is given in table 1. In each case measurements of aerodynamic force and moment components were made over the yaw angle range -5 to 20 degrees, which enabled a wind averaged drag coefficient (C_DWAV) to be evaluated. For a comparison, a datum, or baseline, vehicle was chosen as configuration 04. This corresponds to the 'streamlined' taker set at mid incidence with the complete set of accessories (hatches, ladders, crash bars and trailer stand).

4.2 Flow visualisation studies

An initial series of tests were carried out to assess the sensitivity of the flow visualisation technique to changes in vehicle geometry. This was followed by a systematic study using the baseline vehicle of the dispersion of a smoke plume (released from either the front, centre or rear wheel arch) at stations on the vehicle longitudinal axis from four body widths upstream of the tanker base to two body widths downstream, depending on the location of the source under investigation. In all the cases, tests were carried out with the vehicle at zero yaw and the smoke was released from one side, the offside, only.

5. RESULTS

5.1 Aerodynamic force and moment measurements

The force and moment coefficients for each of the 36 model configurations tested are tabulated in Appendix A. Coefficients are based on a model reference frontal area (A) of 0.098 m^2 and a reference length (in this case model width) of 0.26m. All tests were made at a nominal flow velocity of 55 m/s which corresponds to a Reynolds number of $\approx 1.1 \times 10^6$, approximately 1/5th of the full scale Reynolds number at 55 mph.

All wind tunnel results have been corrected for the effects of (a) tare/strut interference and (b) working section blockage, according to Carr (6).

A summary of the aerodynamic drag data for each configuration is given in table 2. Values of drag coefficient at zero yaw, $C_D(\beta=0)$, and wind averaged drag C_DWAV, are given together with the corresponding percentage change in these values relative to that of the baseline/datum configuration 04. Wind averaged drag coefficients have been evaluated according to Ingram (7).

Graphical presentation of the results is as follows:

(i) drag coefficient versus yaw angle; figures (15) - (21).

(ii) change in drag coefficient, as a percentage of the drag coefficient of the baseline vehicle, versus yaw angle; figures (22) - (32).

(iii) the percentage variation in wind averaged drag coefficient for different vehicle configurations; figures (33) - (39).

(iv) variation of lift coefficient versus yaw angle; figures (40) and (41).

5.2 Flow visualisation studies

Assessment of the plume dispersion is made by photographing the smoke filament as it is illuminated by a light sheet in a plane normal to the freestream flow direction. Due to the unsteady nature of the flow, several photographs were taken at each condition to obtain a realistic mean. In order to simplify the presentation of this data a schematic representation of the illuminated plume has been prepared which corresponds in each case to the mean location of the edge of the plume, geometrically scaled to the view of the rear of the tanker when looking upstream.

The location of the illuminating light sheet is expressed in terms of vehicle body width (w) upstream (-ve. w) and downstream (+ve. w) of the vehicle base. It was found that measurements taken more than 2 body widths downstream of the vehicle were difficult to interpret due to diffusion of the smoke filament.

6. DISCUSSION OF RESULTS

6.1 Aerodynamic drag characteristics of the baseline vehicle

The relatively streamlined shape of the Leyland T45 tractor unit would suggest that changes in tanker forebody shape would have an effect on overall vehicle drag. It is shown that the drag coefficient at zero yaw, $C_D(\beta=0)$, increases by 7% for the square edged tanker with a corresponding increase in wind averaged drag, C_DWAV, of 5%. This influence of tanker end shape on drag is reflected throughout the tanker incidence range, see figures (15) and (22). It is assumed that the main factor contributing to the change in drag is the increased curvature of the container forebody, although rounding the base of the tanker may also be significant. It is not possible from these data to distinguish between the two effects.

The incidence of the tanker influences the drag of the vehicle primarily in relation to the extent to which the tanker forebody is exposed to the freestream flow. The magnitude of the drag change is understandably dependent on the shape of the tanker forebody, the drag of the 'streamlined' tanker being less incidence dependent than the square tanker, see figure (24). Surprisingly, the percentage drag change for a given tank incidence is almost constant across the yaw angle range. This results in significant changes in wind averaged drag, see figure (33).

As would be expected, the ancillary components mounted on the tank and trailer result in a higher wind averaged drag coefficient, see figure (34). Changes in drag coefficient at zero yaw are very small but become significant as the yaw angle is increased, see figure (17). Variations in drag are not symmetrical about zero yaw as the ladders are only mounted on one side of the tank, see figures (25) and (26). In general, (i) the effect of the ancillary components is more significant on the streamlined tanker, which has a greater amount of attached flow, and (ii) the ladders and hatches develop more drag because they are exposed to flow with a much higher local velocity.

6.2 Variations in drag due to trailer skirts

As in previous investigations on articulated vehicles, the use of trailer skirts is seen to make significant reductions in wind averaged drag. In the case of

the tanker vehicle, changes in C_DWAV of between 7% and 9% were measured depending on the type of skirt being used, see figure (36). The magnitude of the drag reduction is perhaps slightly higher than that measured for similar devices on conventional articulated box container vehicles. This is explained by the reduction in drag offered by the tanker vehicle skirts at low, even zero, yaw angle, see figures (27) to (29). (Trailer skirts on conventional articulated vehicles have been seen to have little effect on drag at zero yaw).

The complex nature of the flow in the region of the skirts is further emphasised by the fact that covered skirts result in a larger drag reduction than open skirts, particularly at low yaw angles. This results in a greater reduction in wind averaged drag for covered skirts.

The differences in drag reduction due to full or partial skirts are surprisingly small. This is assumed to be due to the fact that although the partial skirts leave the trailer wheels exposed, these wheels are fixed in the wind tunnel simulation and therefore the flowfield associated with them would be considerably different to that expected full scale. This means that a critical assessment of the effectiveness of skirts in the vicinity of the trailer wheels is extremely difficult for a relatively simple wind tunnel simulation of the type reported here.

The shortened partial covered trailer skirts, configuration 30, were tested in order to assess a practical skirt arrangement which could be mounted on the existing crash bar and wheel arch assembly. The resulting reduction in C_DWAV of $\approx$ 3% is considerably smaller than that given by partial skirts, $\approx$ 6%. This reduction in performance is assumed to be due to: (i) the reduced skirt area, since previous investigations have shown the effectiveness of skirts to be almost directly proportional to their size, and (ii) the moulding used to streamline the front of the skirt, see figure (9), which may constitute additional drag.

6.3 Drag reduction due to tractor-trailer gap flow control

The flow in the gap between the rear of the tractor and the trailer forebody is known to play a significant part in the development of the overall vehicle flowfield. At low yaw angles the flow direction is predominantly from top to bottom - this relatively high speed air meets the flow from under the vehicle and consequently moves out sideways, increasing the effective wake of the

vehicle. At higher yaw angles the flow in the gap is dominated by a lateral movement of air from the windward to the leeward side of the vehicle - this flow effectively increasing the size of the vehicle wake in a similar way to the low yaw angle case.

The aim of gap seals is simply to restrict this flow and consequently stabilise the wake in that region. It would be expected that a vertical gap seal is more effective at higher yaw angles. This is apparent from figures (19) and (31), but the corresponding reduction in wind averaged drag, see figure (37), is very small. It would appear that vertical gap seals are much more effective on box container vehicles than on tankers.

In contrast, the horizontal gap seals are significantly more effective at yaw angles less than 10 degrees, figure (30), giving a 12% reduction in C_D at zero yaw, and a negligible effect at 15 degrees yaw. Nevertheless, the wind averaged drag data for horizontal seals emphasises the effectiveness of this type of device with reductions of 7% and 6% for large and small seals respectively, figure (37). The relatively small effect of the size of the seal is important in that it is suggesting that the majority of the flow in the tractor-trailer gap is concentrated on the forebody of the trailer. Consequently it is the positioning of these flow devices (relative to the stagnation point) and not necessarily their size which determines their effectiveness.

6.4 Drag reducing effectiveness of cab roof fairings

The most widely used add-on devices for reducing the drag on articulated tractor-trailer vehicles is the cab roof mounted fairing. It has been shown from previous work, see Cowperthwaite (3) and others, that the design of the fairing is important in that it is intended to 'match' the flow of the tractor unit to that of the trailer. Clearly, the flowfield around a tanker trailer is different to that on a box container - for which the majority of cab roof fairings have been designed - and it was considered important to assess their drag reducing effectiveness when used with tankers.

The fairing chosen was intended to model the commercially available fairing for the Leyland T45 tractor and as such reflects the type of unit currently in use. It was seen to reduce the zero yaw drag coefficient, $C_D(\beta=0)$, by between 2% and 3% depending on the tanker incidence. However, its effectiveness fell off

sharply at yaw angles greater than 3 degrees, see figure (32), resulting in an increase in drag coefficient. Consequently the wind averaged drag was increased, irrespective of the tanker incidence. This has been shown by Cowperthwaite (3) to be due to the drag of the roof deflector itself at higher yaw angles for box container vehicles. This is emphasised in the case of the tanker vehicle by the relatively smaller drag penalty attributable to the tanker trailer at high yaw angles.

The significance of the design of the fairing itself prompted a series of tests on a new style of 'tanker' cab roof mounted fairing which was intended to more closely accommodate the flowfield around the tanker forebody. The principle differences between the 'standard' and 'tanker' fairings are: (i) a reduced frontal area, since the tanker forebody does not protrude above the line of the cab roof as far as would be expected for a box container, and (ii) a rounded cross section to match the flow to that of the round trailer.

The results show the significance of these design changes; reductions in zero yaw drag coefficient of 15% - 16% were obtained, depending on tanker incidence. This effectiveness was maintained at higher yaw angles resulting in reductions in wind averaged drag (C_DWAV) of between 8% and 9.5%, figure (38). Clearly, accurate matching of the flowfield is important. It is possibly even more critical than for a comparable box container vehicle since the drag penalty due to a mismatch of the flow, see Cowperthwaite (3), would appear to be greater in the case of a tanker vehicle.

A further development of the cab roof fairing was evaluated in which the fairing was extended rearwards and vertical side fairings were added to the cab. This had the effect of reducing the tractor-trailer gap. The results, for configurations 34 to 36 inclusive, suggest that this extended fairing makes the matching of the tractor and trailer flowfields more critical since the magnitude of the zero yaw drag reduction of between 14% and 17% is dependent on tanker incidence to a greater degree than for the simple tanker fairing. Similarly, the reductions in wind averaged drag show a slight improvement on the simple tanker fairing, see figure (39). It would appear therefore that attempts to reduce drag through the use of 'customised' cab roof fairings of this type can be successful but the additional improvement over that obtained for a simple cab roof fairing - providing it is designed specifically for tanker trailers - may be small.

6.5 Analysis of variations in aerodynamic lift coefficient (C_L)

The model mounting technique was modified specifically for the tanker test programme in order to increase the accuracy of aerodynamic lift measurements. This was because it was assumed that the cylindrical shape of the tanker trailer could be producing significantly more lift than its box container counterpart, and that this lift generating flow could be the mechanism responsible for the greater spray dispersion seen on tankers during the preceding trials. If this were true then it would be possible to correlate changes in lift force with changes in spray dispersion.

The magnitude of the lift coefficients measured are typically 1/3rd to 1/2 that of the drag coefficient depending on model configuration and yaw angle. Changes in lift due to the addition of various tanker ancillary components such as hatches and ladders, etc. were negligible, as would be expected. The influence of tanker shape on the lift force only becomes significant at high yaw angles. However, the effect of tank incidence is significant, particularly for the more streamlined tank, see figure (40).

The largest changes in lift were associated with vehicle configurations which used either; cab roof mounted fairings or horizontal tractor-trailer gap seals, see figure (41). In the case of the horizontal gap seals, the reduction in lift at zero yaw was $\approx$ 35% irrespective of the size of the seal. This suggests that the loading on the device itself is small relative to the change in flowfield it induces. A reduction in lift implies an increase in pressure (a reduction in local flow velocity) on the upper part of the vehicle or, vice versa, a decrease in pressure (an increase in local flow velocity) on the underside of the vehicle. In this case, in view of the associated drag reduction, it is more likely that the dominant effect is a reduction in local flow velocity on the upper part of the vehicle. The corresponding increase in pressure in this region is thought likely to deter water spray from being carried vertically from its source at the cab wheels, and therefore to reduce dispersion. Such an assessment can only be a hypothesis without recourse to a detailed analysis of the flowfield, and such an analysis would be subject to Reynolds number and ground effect simulation errors.

A similar mechanism is thought to be responsible for the changes in lift measured for the cab roof fairings. In this case the lift variation is larger than for

the gap seal, ≈ 45% to 52%, and it is assumed that the load on the fairing itself is such as to increase the lift. Therefore the change in flowfield for the vehicle is very significant.

6.6 Wake flow visualisation studies

6.6.1 Initial studies

An initial series of tests were carried out to establish the effectiveness of the experimental technique in analysing changes in the structure of the wake due to modifications to the vehicle. An assessment of the wake was made over a range of axial stations using smoke sources at both 'front' and 'centre' wheel arches, for vehicle configurations with and without: (i) cab roof mounted fairings and (ii) tractor-trailer horizontal gap seals. During these tests it was found to be impossible to distinguish any differences in the wake smoke filament dispersion due to a change in the vehicle configuration.

A similar assessment was made with the smoke source in the rear wheel arch for models with and without trailer skirts of various configurations. The only observable difference in this case was between full and partial skirt configurations, when the smoke was unable to escape from the wheel arch due to the full skirt. The resulting plume was confined to the underbody of the vehicle - a region in which analysis of the resulting plume photograph is very difficult.

It is considered unlikely that modifications to the vehicle which resulted in such relatively large variations in lift and drag forces do not have an observable effect on the structure of the wake or the dispersion of the smoke filament from the area of the wheels. It is possible that the visualisation technique was not sufficiently sensitive to detect these changes. This insensitivity is likely to have been aggravated by: (i) the low Reynolds number ($\approx 0.6 \times 10^6$), at which the flow visualisation studies had to be carried out due to the maximum speed of the wind tunnel and (ii) the relatively crude simulation of ground effect.

In view of this limitation it was decided to use the flow visualisation technique to identify the relative dispersion characteristics of flow emanating from each of the three wheel arch areas for the baseline vehicle, configuration 04, only. Subsequent full scale tests at TRRL suggest that the wind tunnel observations

are correct, and that aerodynamic modifications to the tanker do not affect the subjective appearance of the spray plume geometry.

6.6.2 Wheel arch plume dispersion for baseline vehicle

A schematic summary of the wake flow visualisation using a smoke source in the rear wheel arch is given in figure (42). Analysis using this technique concentrates on the extent to which the dispersing plume moves vertically and laterally with respect to the vehicle, as it is carried downstream. It would appear from figure (42) that a plume released from the rear wheel arch does not rise significantly above the level of the wheel arch and thee initial sideways movement away from the vehicle is reversed when the plume is drawn back into the wake by the relatively low pressure region immediately behind the base of the tanker

A similar schematic summary of the wake flow visualisation using a smoke source in the tractor drive wheel arch is given in figures 43 (a) and (b). The dispersion is seen to follow a similar pattern to that for the rear wheel except that the plume is displaced laterally to a greater extent and only the flow near the vehicle is drawn back into the wake on encountering the low pressure region. This lateral movement makes spray generated by the tractor drive wheels particularly relevant to vehicles passing alongside the tanker.

Smoke plume dispersion from the front wheel arches is shown schematically in figures 44 (a) and (b). The significant difference in this case is that the plume moves vertically to a far greater extent, reaching the full height of the tanker within one trailer width of release.

6.6.3 General comments regarding flow visualisation

Interpretation of the smoke plume flow visualisation require considerable care and three important factors should be considered when making comparison with spray dispersion:

(1) The low Reynolds number at which the flow visualisation tests were carried out may influence the flow, particularly in the gap between the tractor and trailer.

(2) The simplified simulation of ground proximity may well have a significant effect on the flow in, and around, the area of the wheels. The wind tunnel

model wheels were fixed and therefore the influence of the flowfield generated by the rotating wheel has been neglected.

(3) The dispersion of a smoke plume may well be considerable different from that of water splash. The smoke does not simulate the inertial forces which could be an important factor influencing splash dispersion.

Despite these limitations, smoke flow visualisation is considered valuable in focusing the attention on certain aspects of the flow prior to full scale spray dispersion studies. It would appear that spray generated by the front wheel is more likely to be drawn higher into the vehicles' wake, and therefore carry further, than that generated at the other wheels. Similarly, smoke released at the centre wheel arch may be drawn sideways away from the vehicle, at near ground level, to a greater extent than that from the front or rear wheels.

Both these effects need to be confirmed by full scale trials. Ideally by full scale smoke studies initially, to study the effectiveness of the wind tunnel modelling technique, followed by spray trials to assess the limitations of smoke as a simulation for water spray. If specific simulation problems were identified it may be possible to refine the smoke visualisation technique, either by modifying the smoke injection process or by seeding the smoke itself with a heavier than air gas to more accurately model the buoyancy of the water spray. Both these techniques would require a more detailed knowledge of both the nature of the spray itself and the local flow characteristics associated with a wheel arch and rotating tyre.

CONCLUSIONS

An extensive programme of wind tunnel tests using scale models has shown that the aerodynamic characteristics of articulated tanker vehicles are similar in many ways to those of box container vehicles. There are however significant differences which may be important when attempting to modify the vehicle so as to reduce aerodynamic drag and water spray dispersion.

The main feature of the flow is that in the region between the tractor and the tanker. Consequently attempts to reduce the aerodynamic drag of the vehicle should concentrate on controlling the flow in this region and 'matching' the aerodynamic interface between tractor and tanker.

A cab roof mounted fairing designed to reduce the aerodynamic drag of a box container is shown to be ineffective on a tanker. However, significant reductions in drag can be achieved with cab roof mounted fairings by changing the design to more closely reflect the flow associated with the tanker forebody.

Horizontally mounted seals between the tractor and tanker are seen to be more effective than vertical seals. Previous research has shown the opposite to be the case for box container vehicles.

Trailer mounted side skirts are seen to be marginally more effective on tankers than box container trailers in reducing drag. Careful design of the skirts is seen to be worthwhile.

An attempt to simulate the dispersion of water spray generated at the road wheels was made by releasing paraffin smoke from the wheel arches of the model in the wind tunnel. The accuracy of this technique is limited by: (i) the simplified simulation of ground effect and (ii) differences between the behaviour smoke filament and water spray.

Within the limits of this simulation it is possible to identify the likely path of water spray generated at each wheel separately. The flow from the front tractor wheels rises rapidly and remains close to the vehicle, while that from the remaining wheels, and in particular the tractor rear wheels, is predominantly drawn sideways away from the vehicle.

RECOMMENDATIONS FOR FURTHER WORK

The results of the wind tunnel force and moment measurements identify specific devices which offer sufficient reduction in aerodynamic drag to warrant further investigation: horizontal gap seals, cab roof mounted fairings and trailer skirts. The effectiveness of these devices is thought to be dependant on tractor and trailer geometry and further optimisation should be made on a specific vehicle for which correlation on-road trials would be possible. The simplicity of the horizontal gap seal in particular is thought to warrant further development.

The simulation of water spray in wind tunnel tests requires further investigation. The smoke injection technique may be more effective if (a) the smoke filament were seeded with a heavier gas to simulate the buoyancy of the water spray and (b) consideration were given to the injection technique so as to optimise the interaction of the 'spray' with the freestream flow. Both these factors would require a more detailed knowledge of the aerodynamic flowfield in and around the wheel/wheel arch combinations. Access to full scale correlation data would be essential.

ACKNOWLEDGEMENTS

Financial support for this programme was provided by the Department of the Environment and Department of Transport, coordinated by the Transport and Road Research Laboratory, Crowthorne, U.K. under agreement: TRR 842/560 - 'Experimental investigation of water spray dispersion from tanker vehicles'. Results are published by permission of the director.

The author would like to thank members of the contract steering committee for their assistance during the programme and in the preparation of this report, particularly Mr. Alan Naysmith (TRRL) and Mr. Ron Rider (Freight Transport Assc.).

REFERENCES

1. GARRY, K.P. "A summary of the scale model wind tunnel measurements and full scale surface pressure tests on the Leyland T45 and DAF 3300 vehicles used for the TRRL spray dispersion programme". CRANFIELD, College of Aeronautics Report No. 8707, April 1987.

2. GARRY, K.P. and COWPERTHWAITE, N.A. "Full scale and wind tunnel surface pressure measurements on the TRRL spray dispersion programme vehicles". CRANFIELD, College of Aeronautics Report No. 8623, December 1987.

3. COWPERTHWAITE, N.A. "Scale model wind tunnel measurements on the Leyland T45 and DAF 3300 vehicles used for the TRRL spray dispersion programme". CRANFIELD, College of Aeronautics Report No. 8622, October 1986.

4. GARRY, K.P. "Aerodynamic characteristics of current commercial vehicles". CRANFIELD, Aero Contact Report 003/79, 1979.

5. ALLAN, J.W. and LILLEY, G.M. "Reduction of water spray from road vehicles in wet conditions: A further investigation with improved trials, measurement equipment and technique". University of Southampton AASU Memo 80/5, July 1981.

6. CARR, G.W. "Wind tunnel blockage corrections for road vehicles". MIRA Report 1971/4.

7. INGRAM, K.C. "The wind averaged drag coefficient applied to heavy goods vehicles". TRRL Supplementary Report 392, 1978.

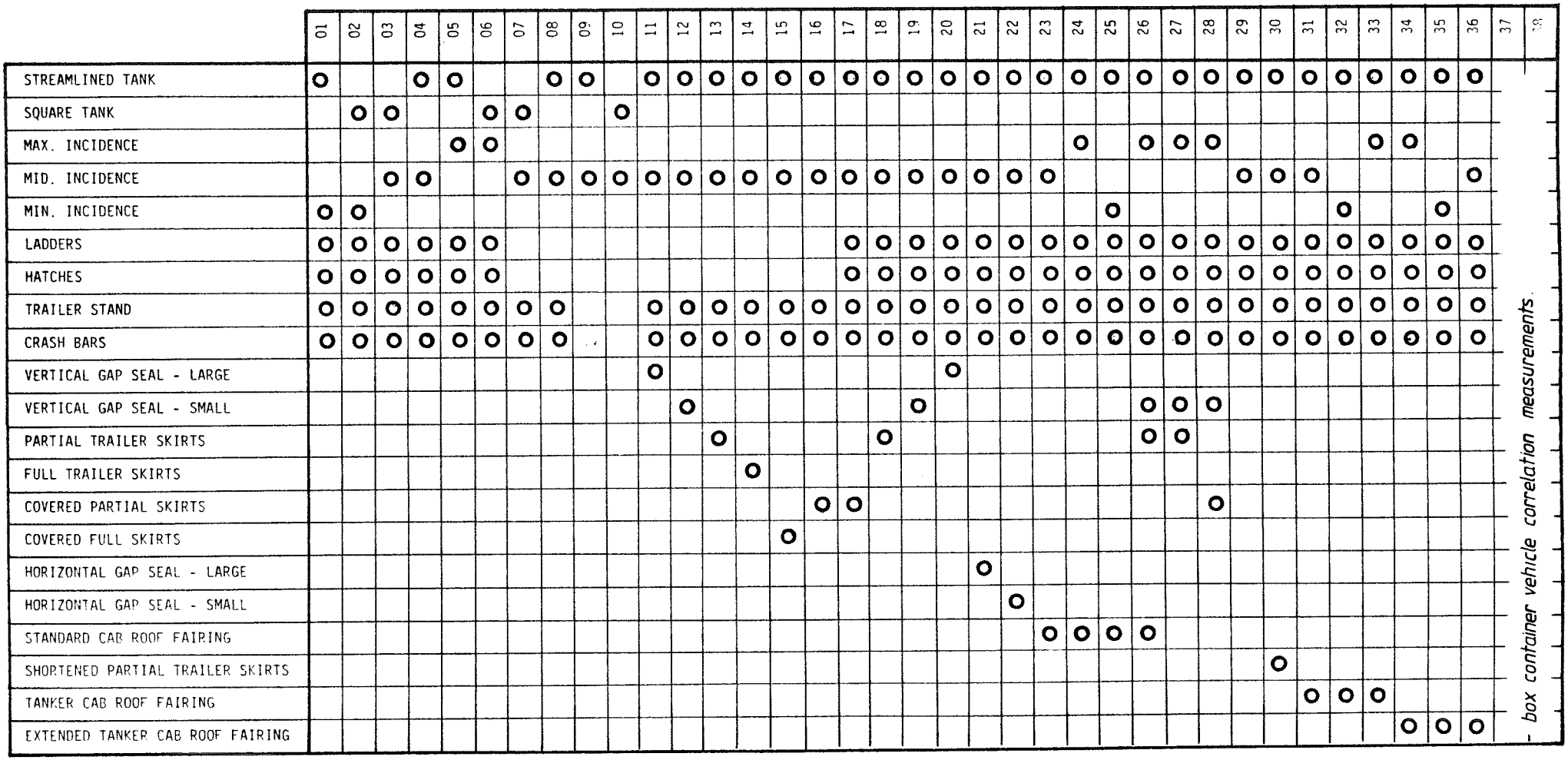

Table 1. Summary of T45 tractor plus tanker wind tunnel model configurations.

CONFIG.NO.	C_D (β=0)	$\%\Delta C_D$(β=0)	C_{DWAV}	$\%\Delta C_{DWAV}$	$\%\Delta C_L$(β=0)
01	0.920	4.56	1.085	6.30	8.4
02	0.990	-2.69	1.176	-1.55	13.5
03	1.030	-6.84	1.218	-5.18	7.4
04	0.964				
05	1.016	-5.39	1.210	-4.49	-10.0
06	1.084	-12.44	1.273	-9.93	-4.8
07	1.015	-5.29	1.184	-2.24	4.1
08	0.943	2.17	1.122	3.10	4.3
09	0.942	2.28	1.108	4.31	0.2
10	1.016	-5.39	1.182	-2.07	1.5
11	0.930	3.52	1.114	3.79	8.4
12	0.944	2.07	1.125	2.84	2.8
13	0.890	7.67	1.076	7.08	-8.2
14	0.885	8.19	1.074	7.25	-10.2
15	0.862	10.58	1.045	9.75	-0.7
16	0.874	9.33	1.055	8.89	5.3
17	0.896	7.05	1.088	6.04	-2.5
18	0.914	5.18	1.113	3.88	-11.0
19	0.962	0.20	1.153	0.04	3.5
20	0.956	0.80	1.149	0.07	4.3
21	0.849	11.92	1.076	7.08	34.6
22	0.845	12.34	1.084	6.39	35.6
23	0.937	2.80	1.181	-1.98	47.9
24	0.935	3.00	1.182	-2.07	45.6
25	0.941	2.38	1.183	-2.15	52.0
26	0.887	7.98	1.137	1.81	45.6
27	0.919	4.66	1.124	2.93	-7.4
28	0.902	4.56	1.099	5.09	3.5
29	0.960				
30	0.916	4.97	1.093	3.30	-2.8
31	0.808	16.18	1.036	8.35	46.2
32	0.814	15.56	1.022	9.57	46.8
33	0.812	15.76	1.043	7.72	45.7
34	0.821	14.83	1.033	8.59	38.0
35	0.799	17.11	1.020	9.76	44.5
36	0.807	16.28	1.026	9.27	42.8
37	1.159	11.46	1.404	-7.41	45.3
38	1.141	12.83	1.366	-9.92	46.1
39	1.309				

(all percentage changes refered to baseline vehicle configuration 04)

Table 2. Summary of aerodynamic lift and drag coefficient data.

LIST OF FIGURES

26. The influence of ancillary components for the streamlined tanker on drag coefficient (C_D).

27. Comparison of partial and full open trailer skirts.

28. Variation of drag coefficient with open or covered full trailer skirts.

29. Comparison of open and covered partial trailer skirts.

30. The influence of tractor cab to tanker forebody horizontal gap seals on drag coefficient (C_D).

31. The influence of tractor cab to tanker forebody vertical gap seals on drag coefficient (C_D).

32. The influence of changes in tanker incidence on drag coefficient for a vehicle fitted with a cab roof fairing.

33. The effect of tank incidence and geometry on wind averaged drag.

34. The effect of tank accessories on wind averaged drag.

35. The influence of tank incidence on wind averaged drag with the standard cab roof fairing.

36. The influence of skirt geometry on wind averaged drag with a rounded tank.

37. The effectiveness of tractor trailer gap seals on wind averaged drag for the rounded tanker.

38. The influence of tank incidence on wind averaged drag for the tanker cab roof fairing.

39. The influence of tank incidence on wind averaged drag for the tanker cab roof fairing with side extensions.

40. The influence of (a) incidence and (b) tanker end shape on lift coefficient (C_L).

41. The influence of (a) cab roof mounted fairings and (b) horizontal gap seals on lift coefficient (C_L).

42. Baseline vehicle wake flow visualisation smoke source in rear wheel arch.

43. Baseline vehicle wake flow visualisation smoke source in centre wheel arch.

44. Baseline vehicle wake flow visualisation smoke source in front wheel arch.

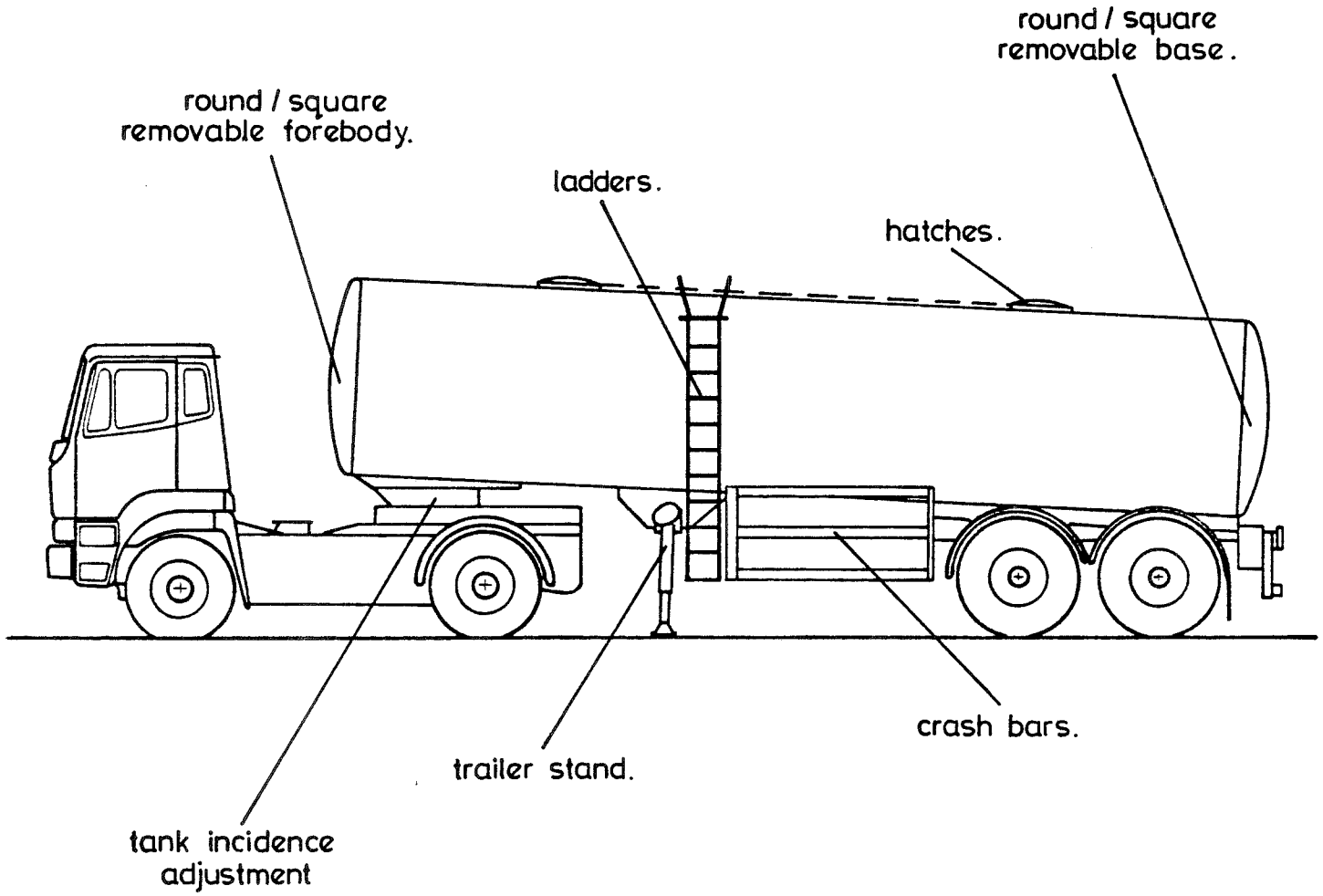

Figure 1. Arrangement of the $^{1}/_{8}^{th}$ scale T45 and articulated tanker wind tunnel model, showing removable/adjustable features.

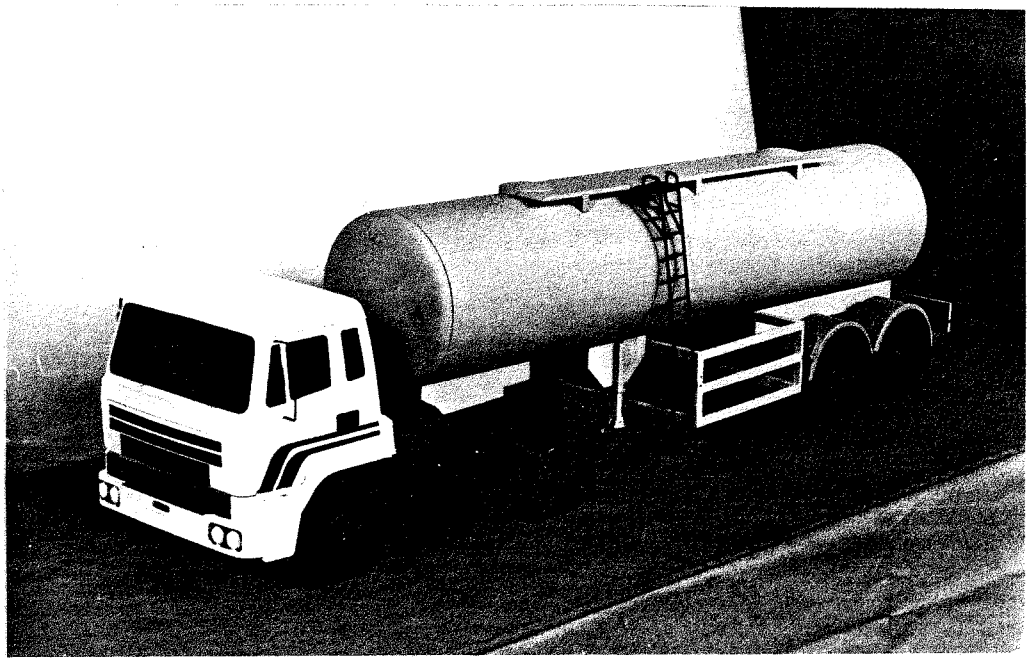

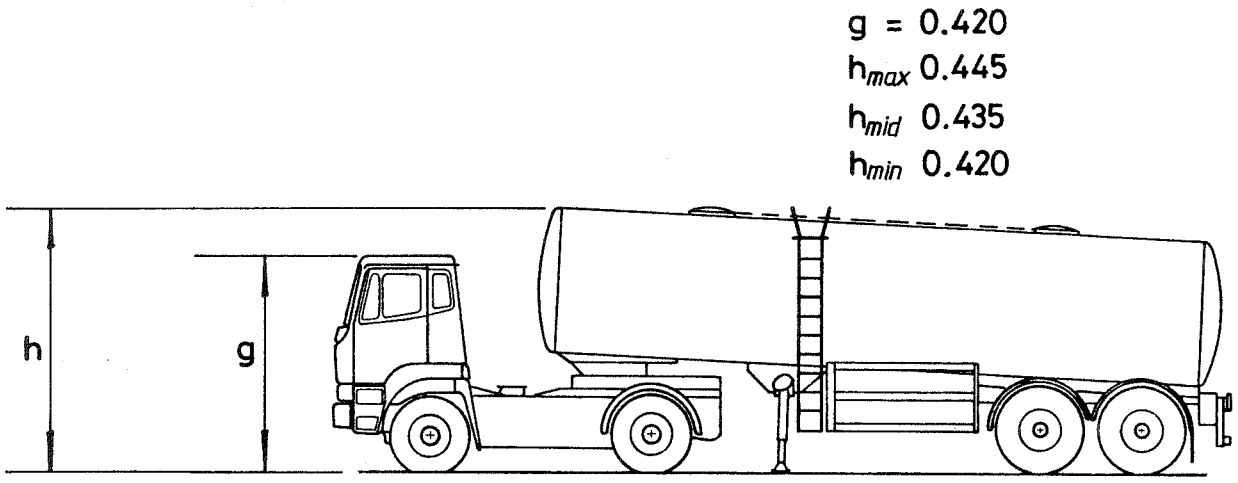

Figure 2. The baseline T45 tractor and articulated tanker model.

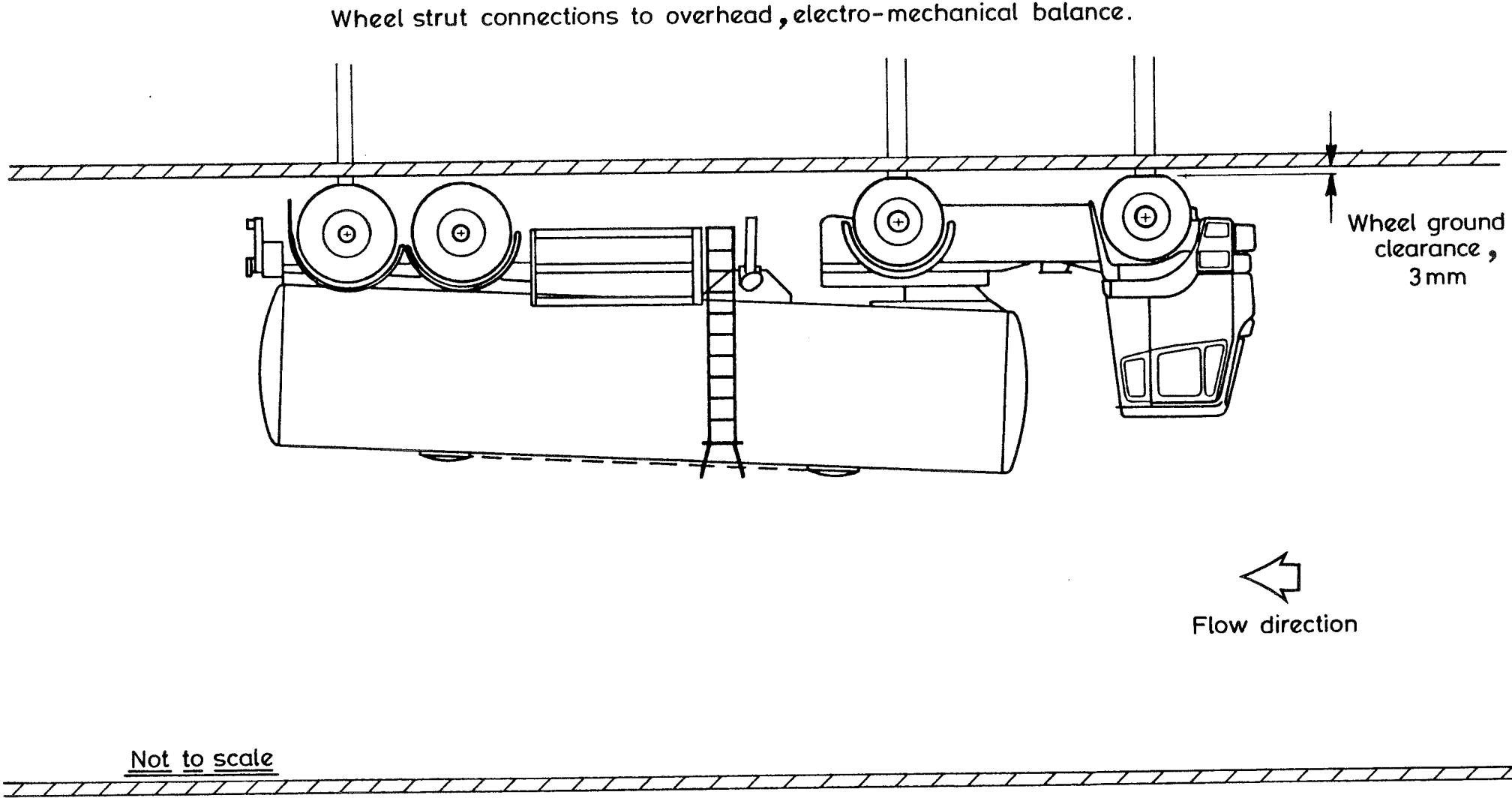

Figure 3. Layout of tanker model mounting system for the 8'x 6' wind tunnel.

College of Aeronautics
Cranfield

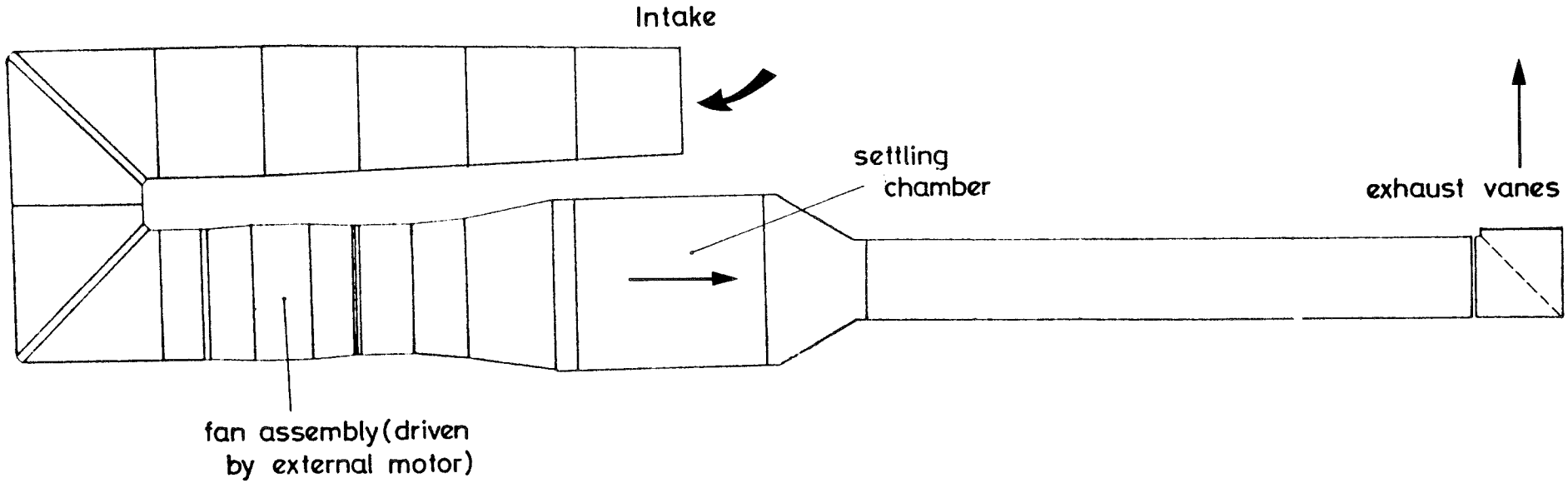

Figure 4.
Arrangement of the 8' x 4' boundary layer wind tunnel .

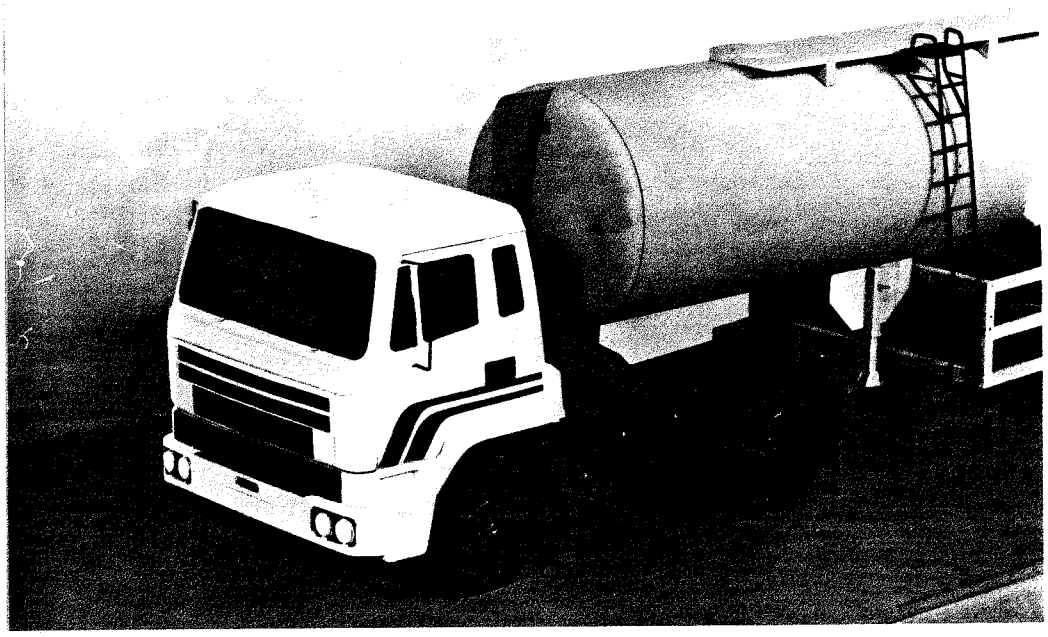

Figure 5. Vertical gap seal.

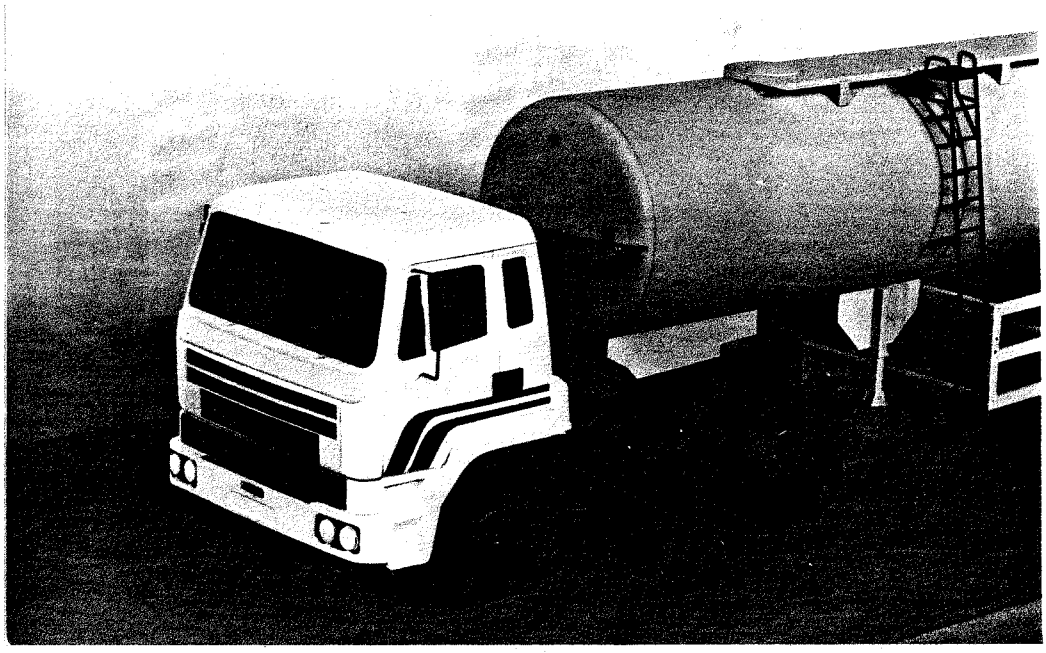

Figure 6. Horizontal gap seal.

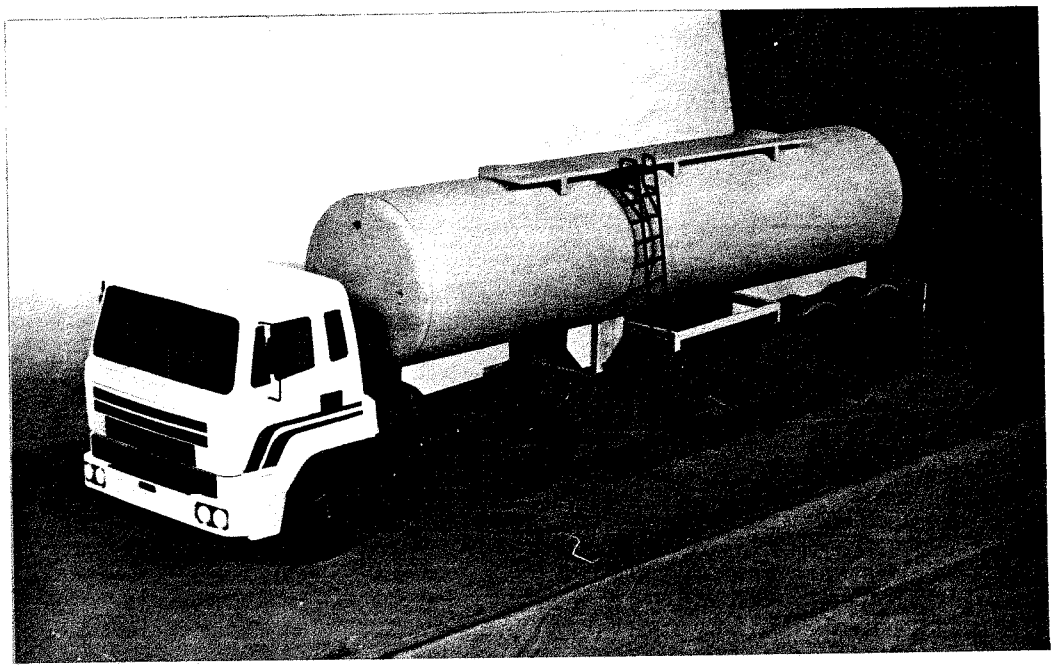

'Open'

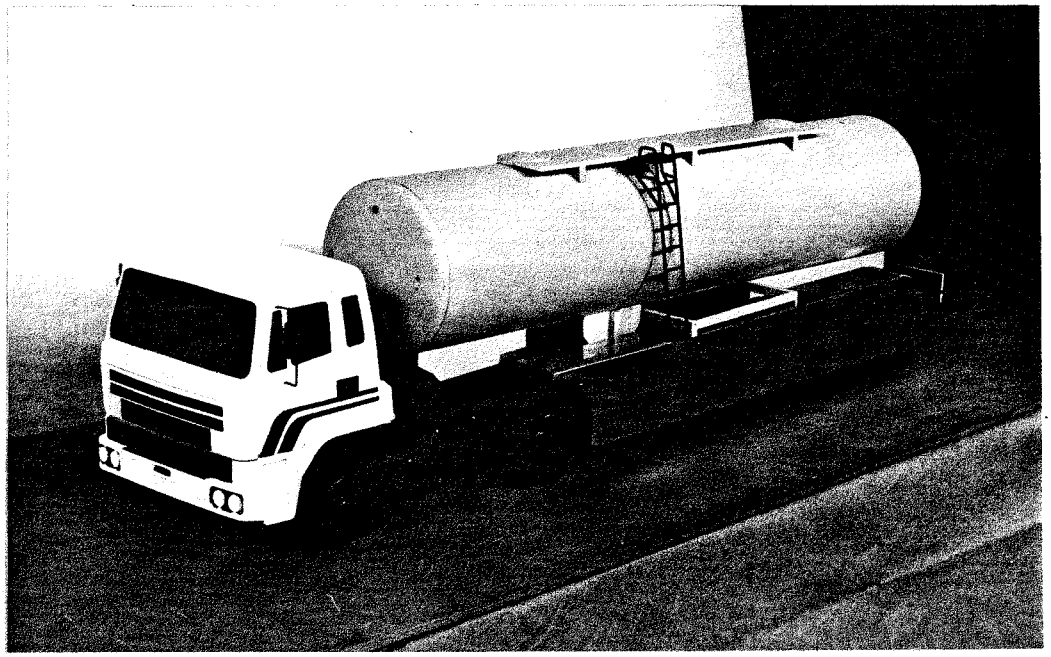

'Covered'

Figure 7. Full trailer skirts.

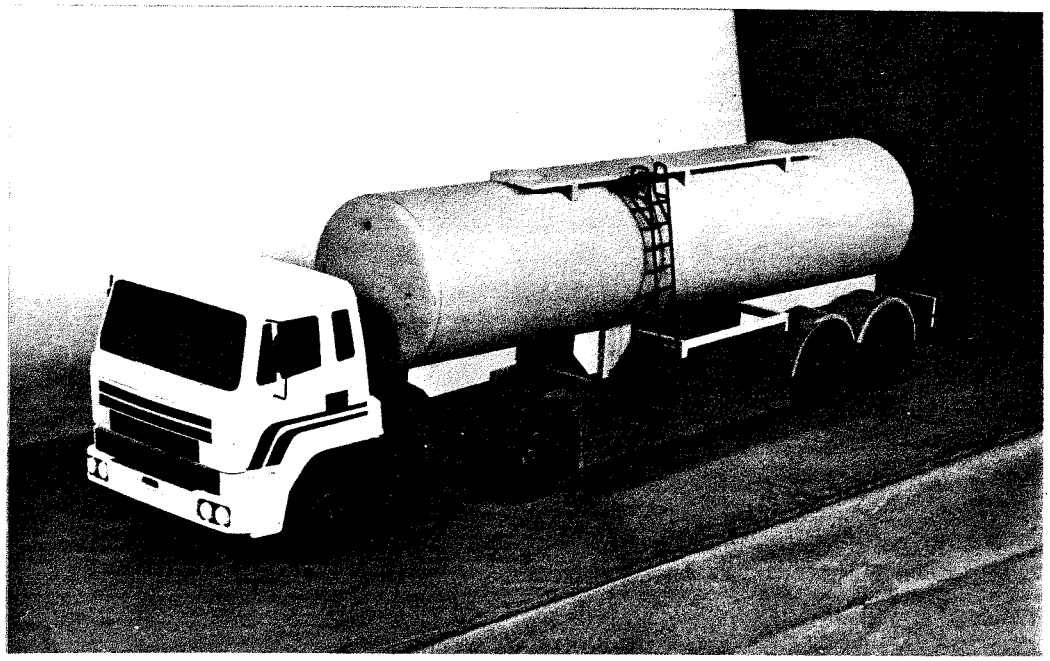

'Open'

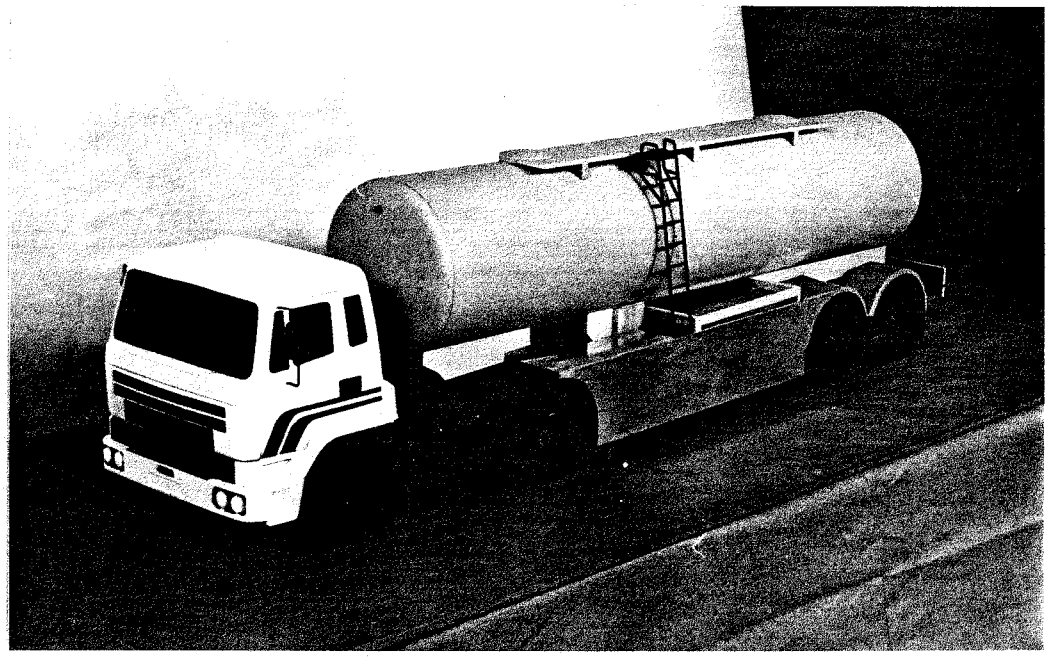

'Covered'

Figure 8. Partial trailer skirts.

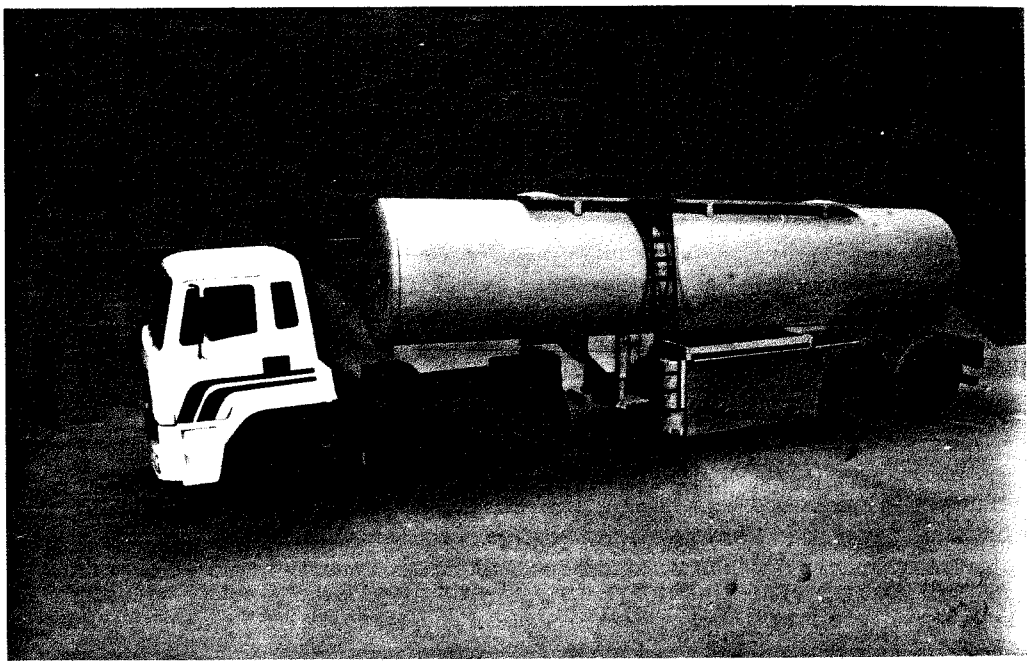

(Streamlined
tanker)

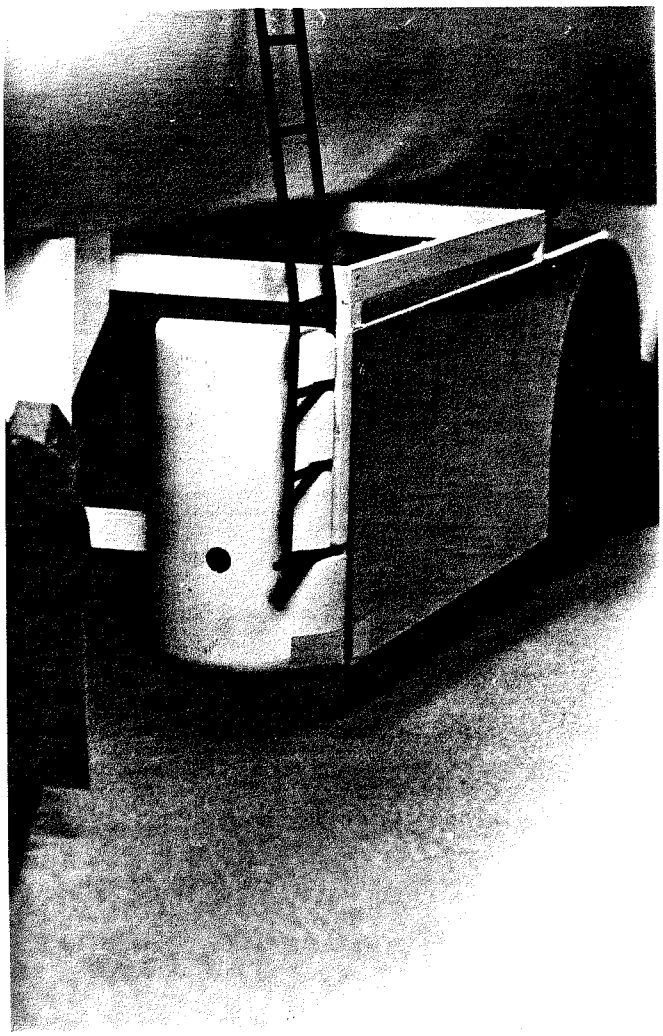

Figure 9. Shortened partial trailer skirts.

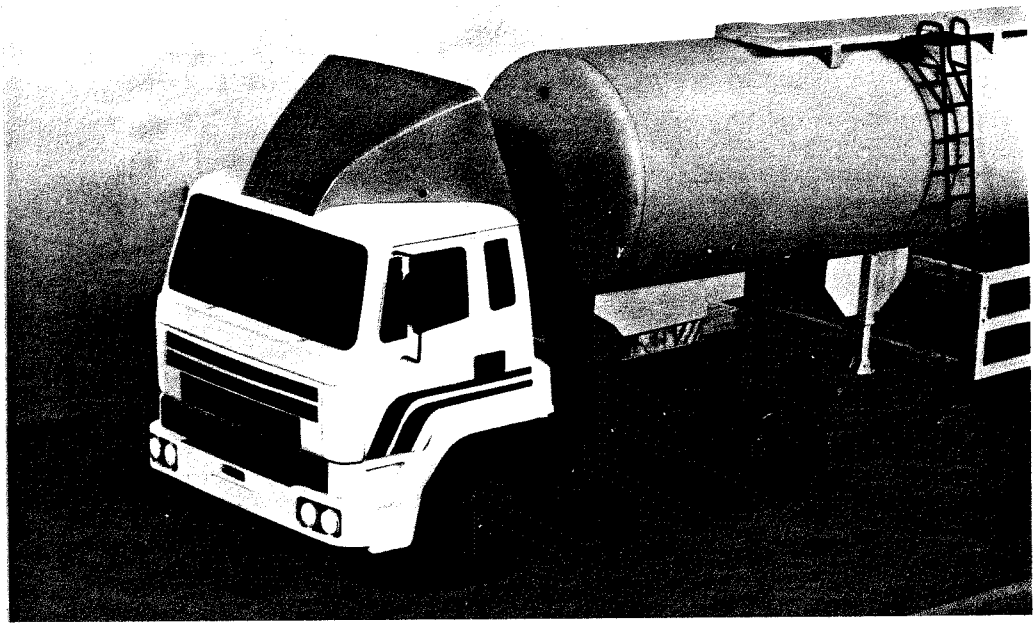

(Maximum incidence)

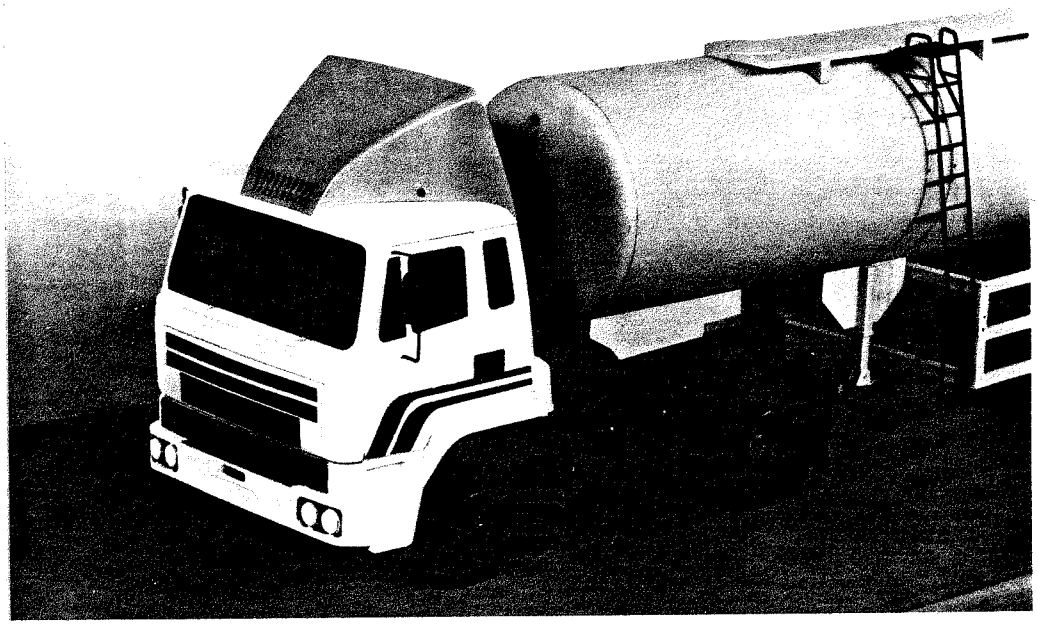

(Minimum incidence)

Figure 10. Standard cab roof fairing.

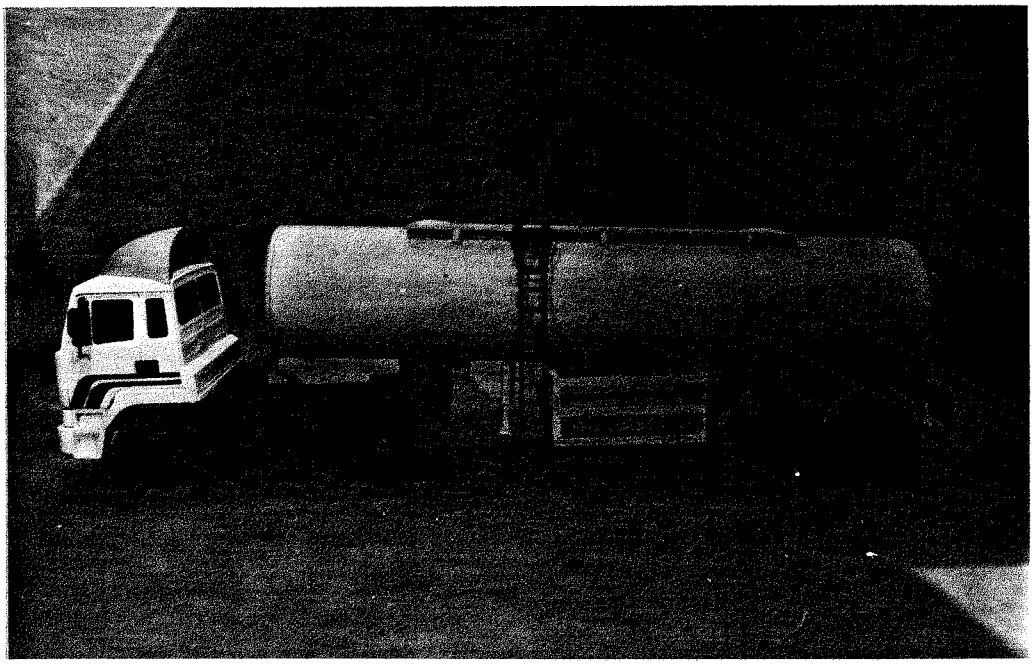

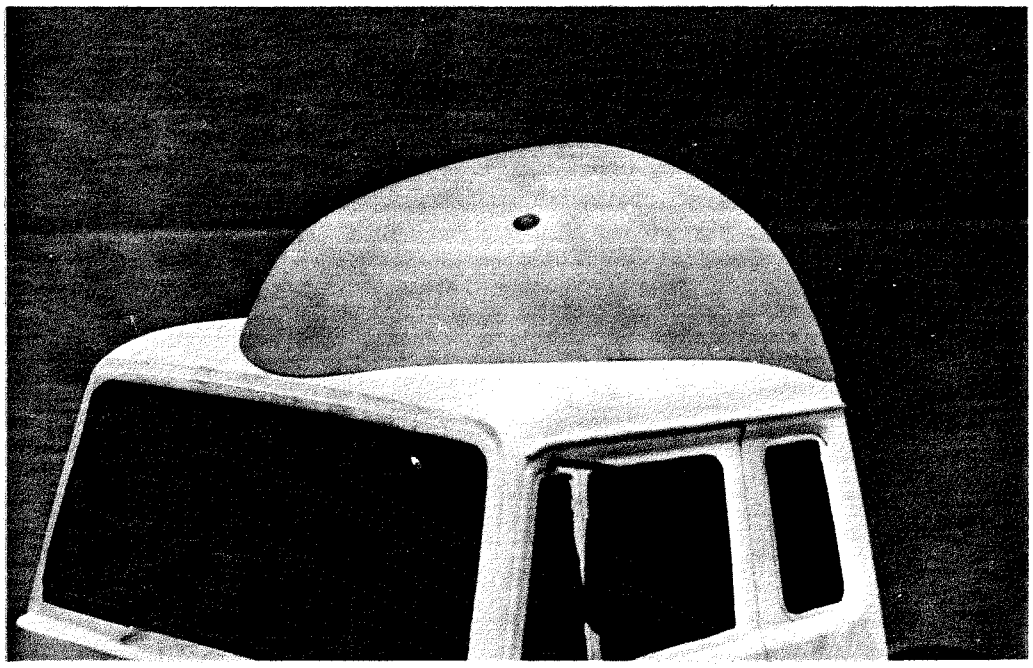

Figure 11. Tanker cab roof fairing.

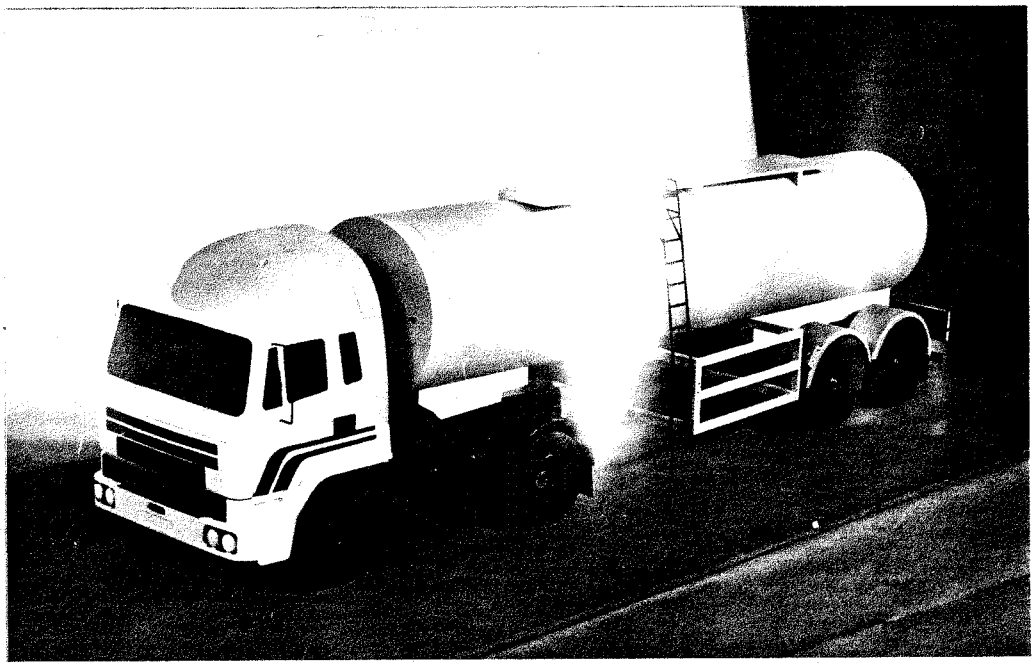

(Extended cab roof fairing with 'square' tanker at minimum incidence)

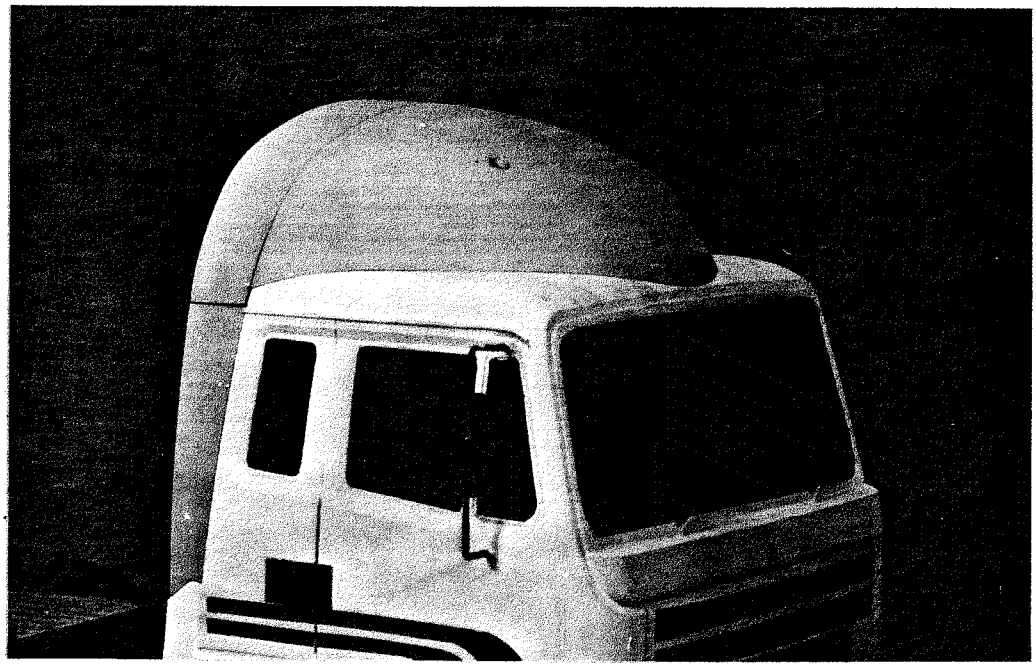

Figure 13. Extended cab roof fairing.

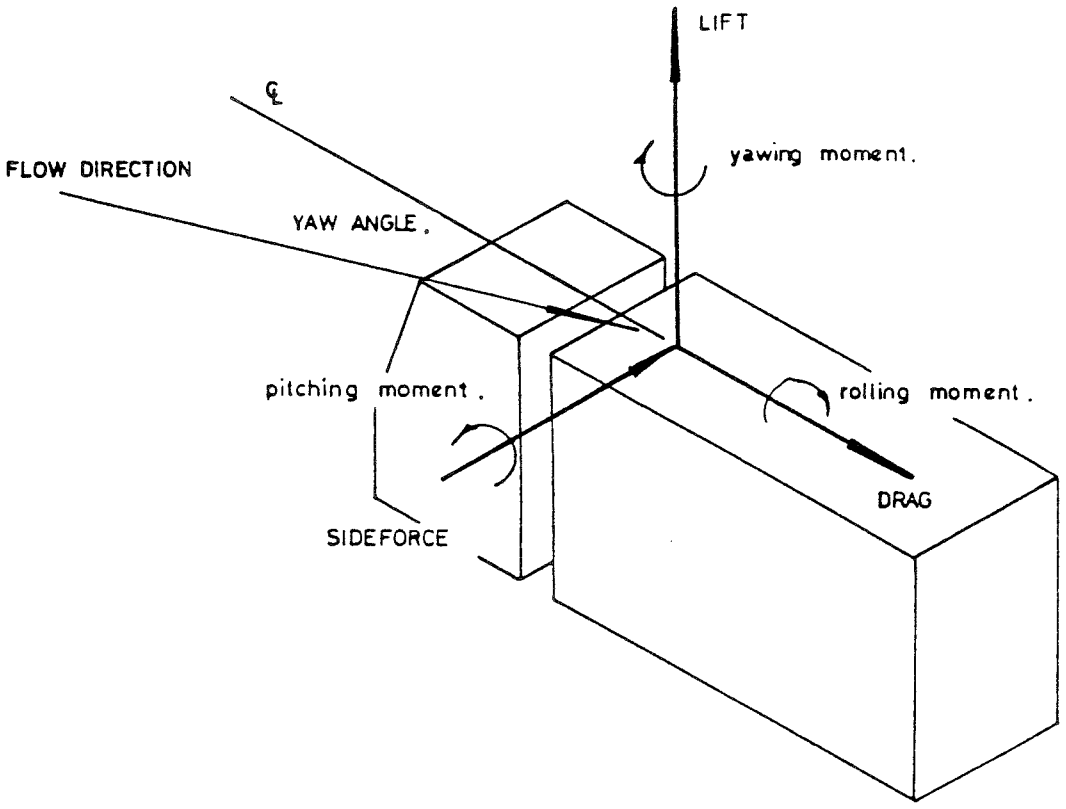

Figure 14.
Aerodynamic Force and Moment Sign Convention.

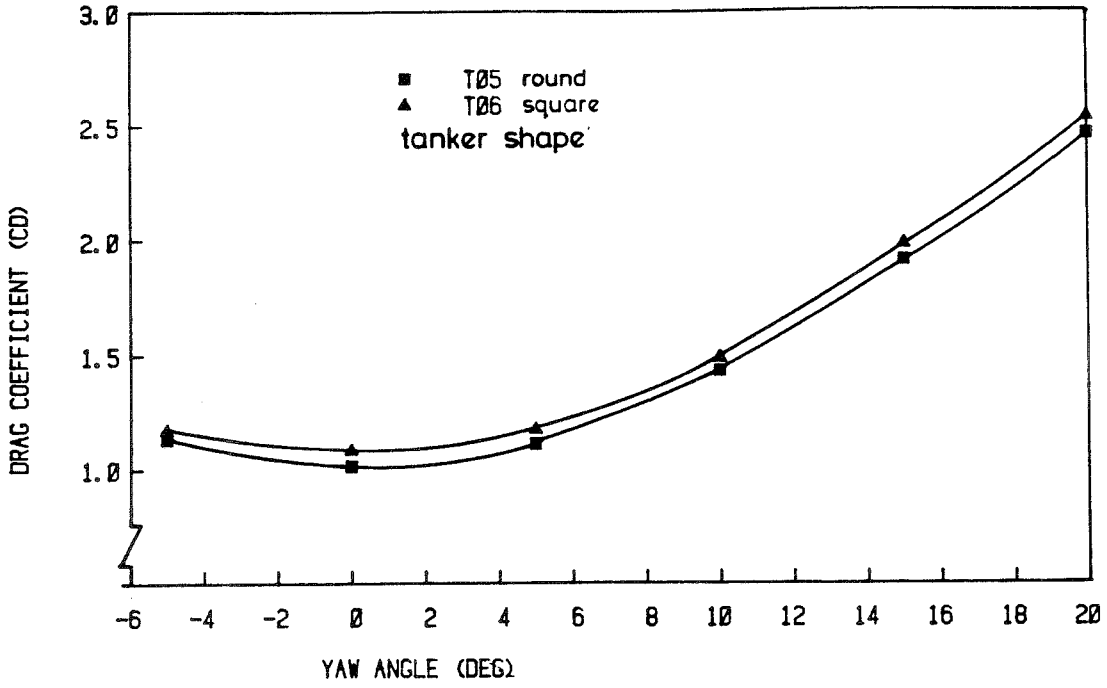

Figure 15. The influence of tanker forebody / base shape on drag coefficient (C_D).

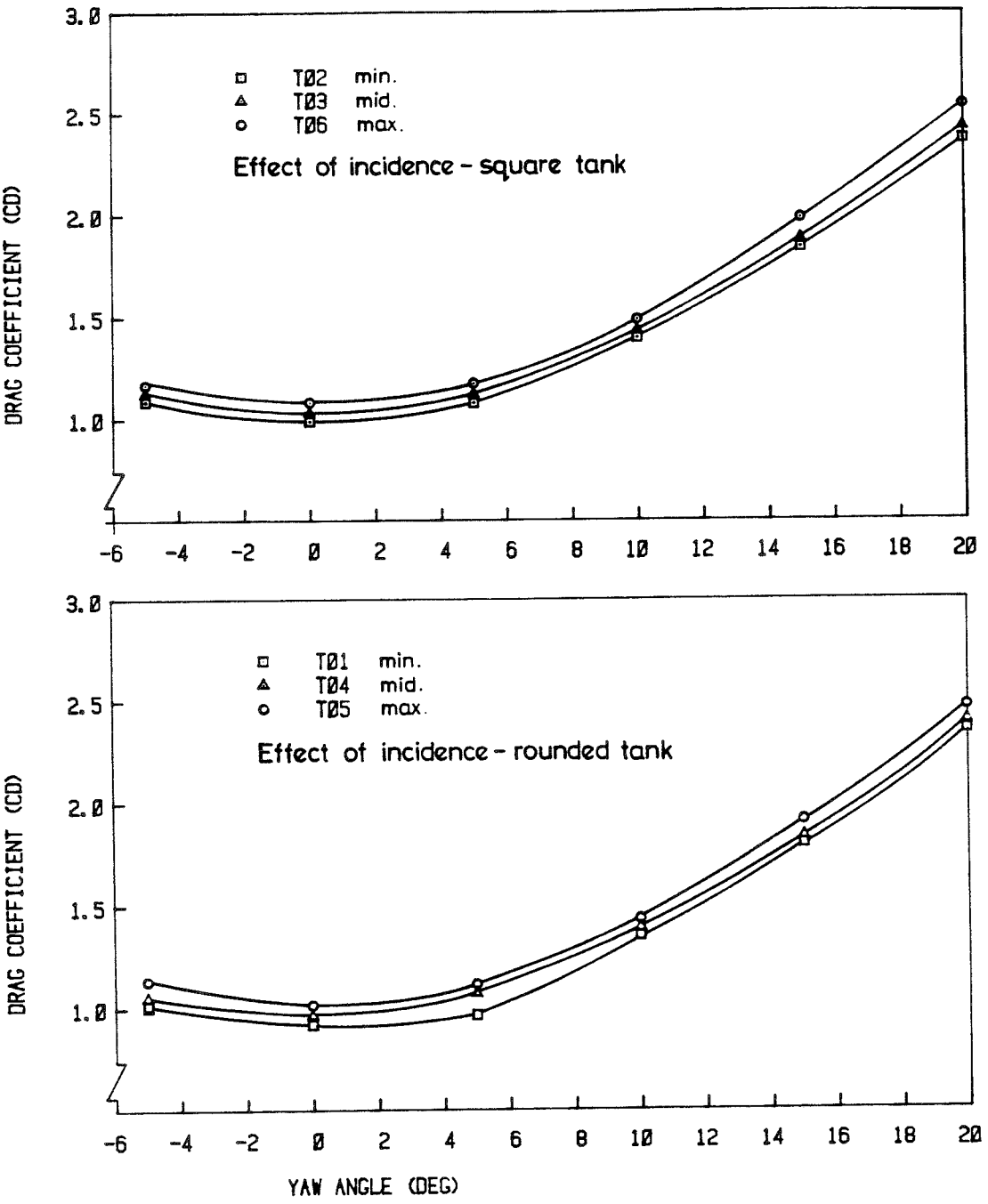

Figure 16. The effect of tank incidence and forebody / base shape on drag coefficient (C_D).

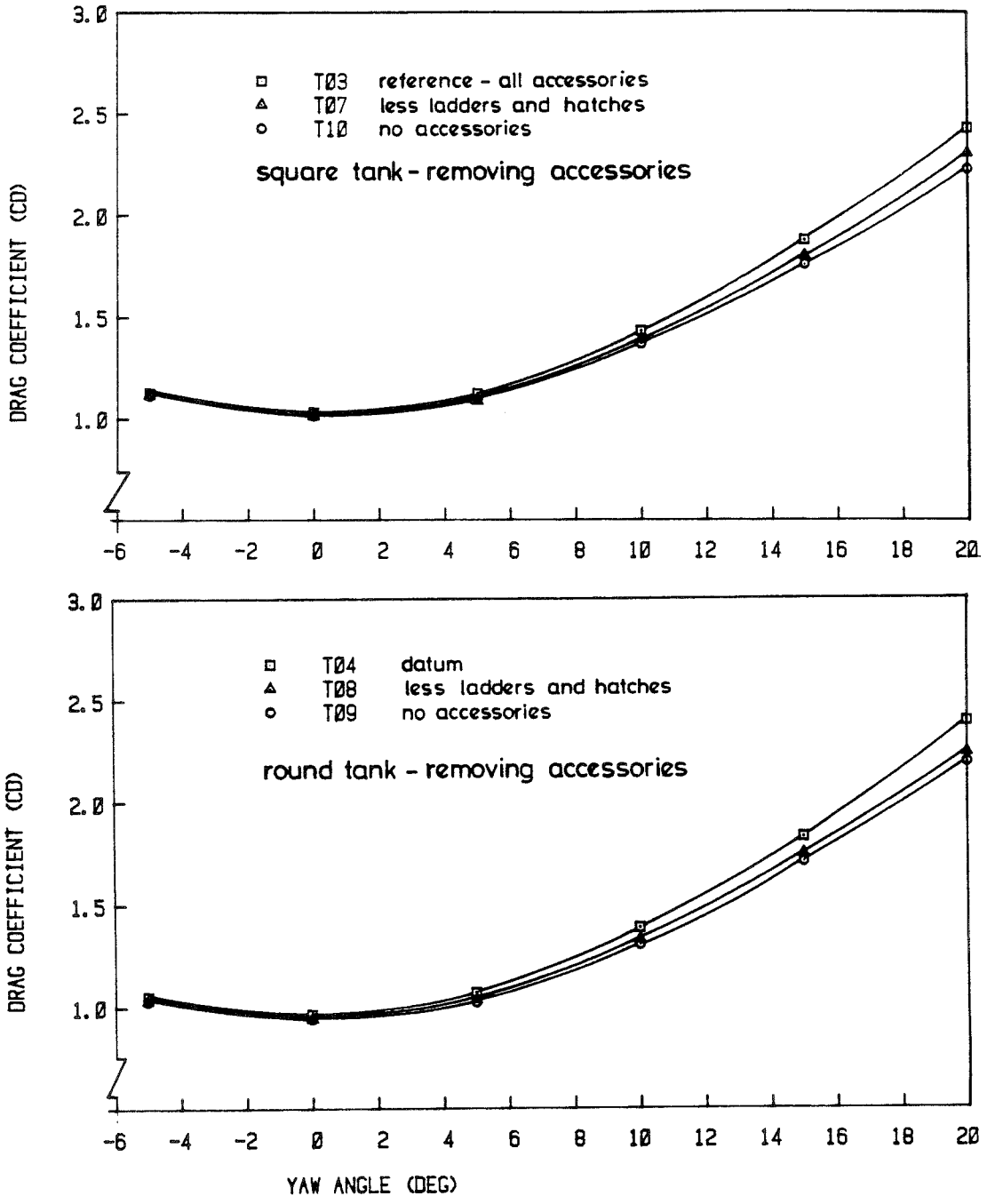

Figure 17. The influence of the tanks ancillary components on drag coefficient (C_D).

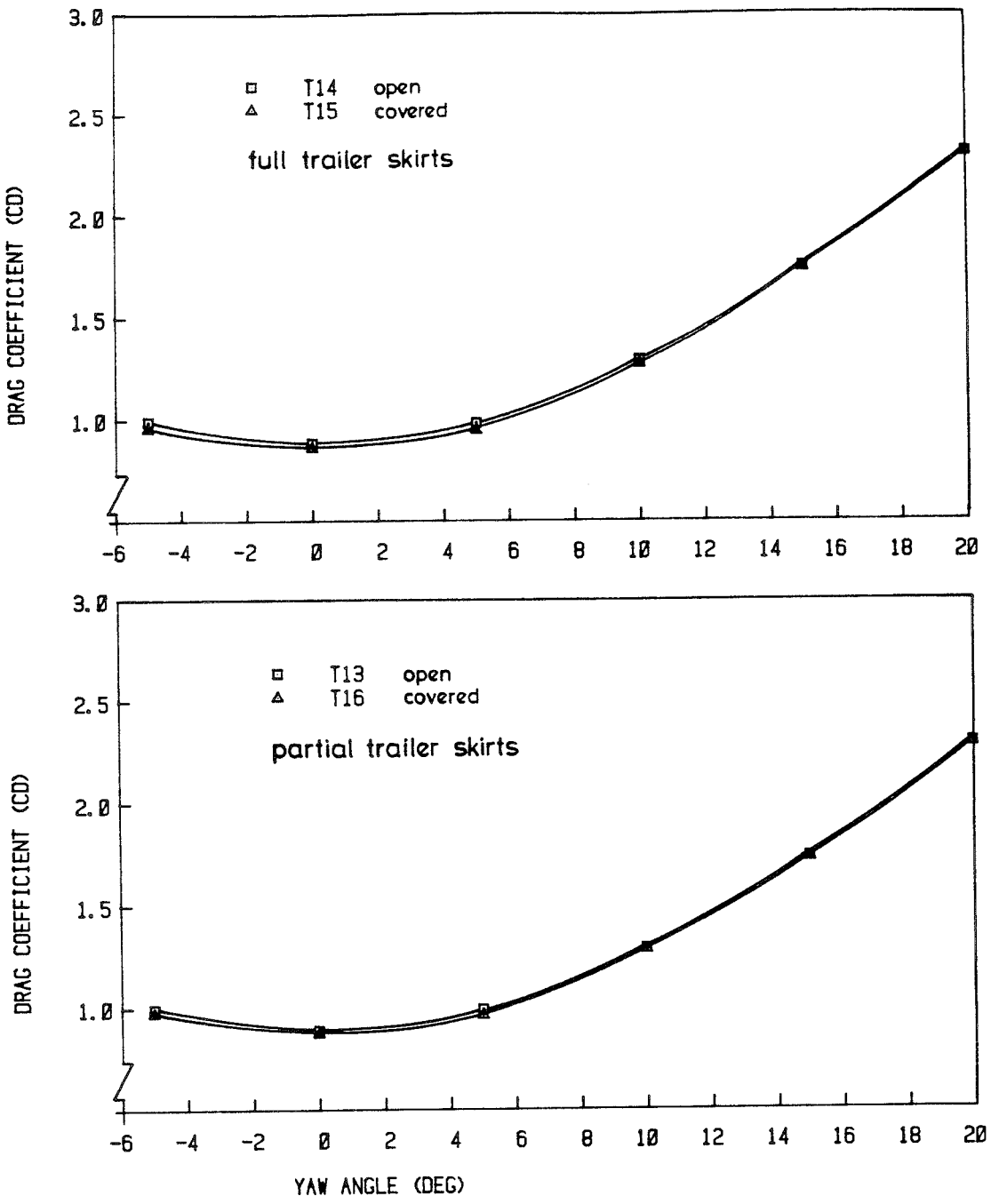

Figure 18. The influence of open or covered full and partial trailer skirts on drag coefficient (C_D)

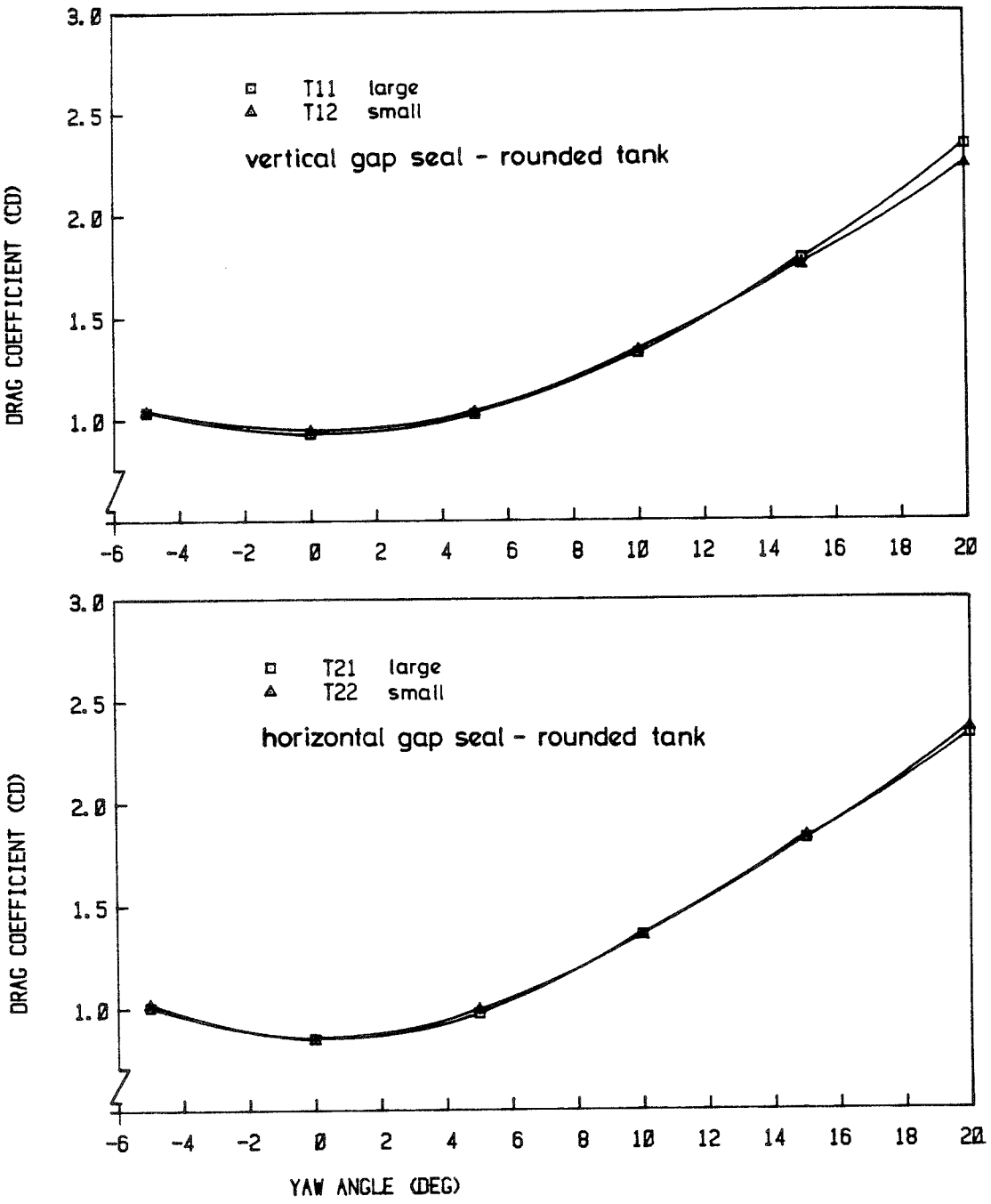

Figure 19. The influence of tractor cab to trailer forebody gap seals on drag coefficient (C_D).

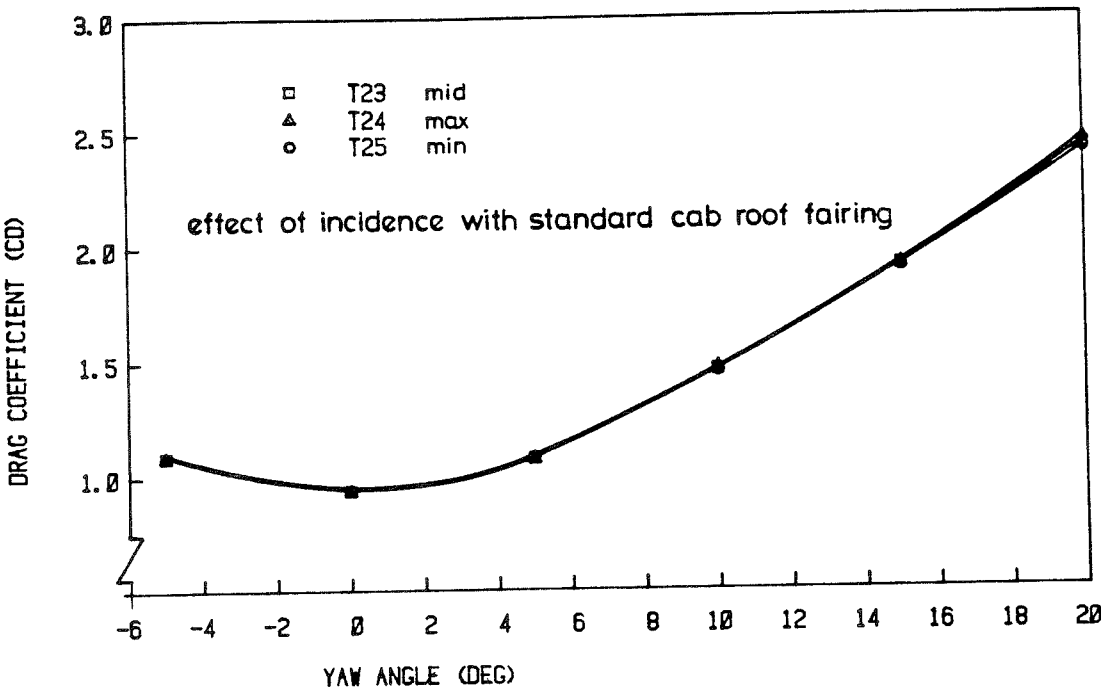

Figure 20. The effect of varying tank incidence with the standard cab roof fairing.

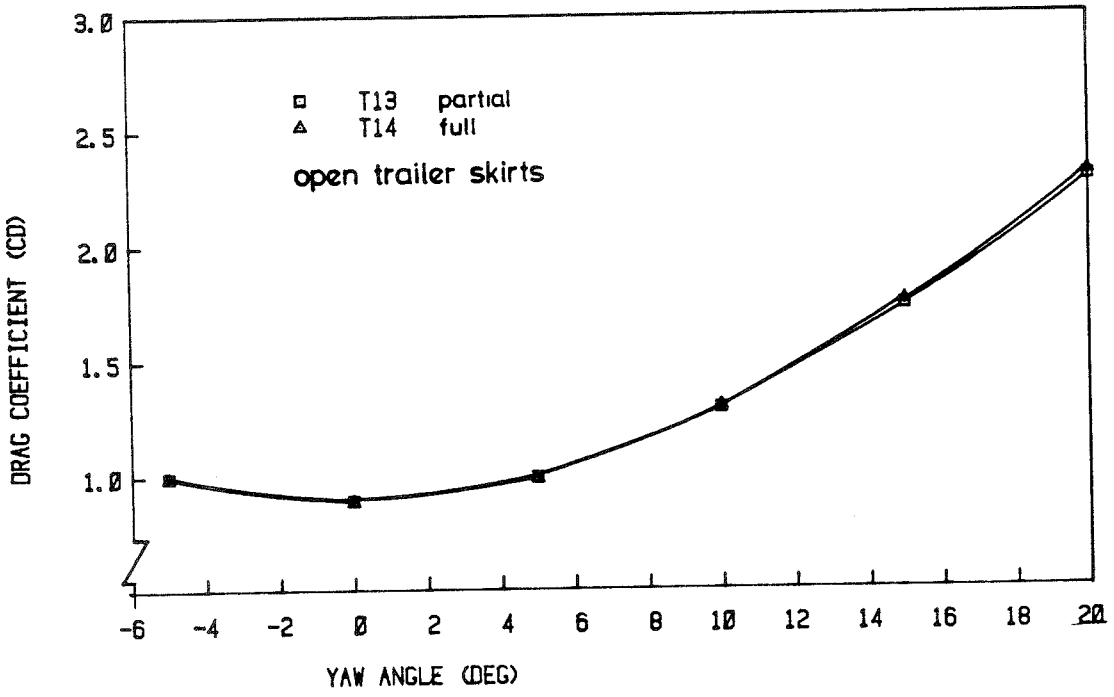

Figure 21. Comparison of the influence of partial or full open trailer skirts on drag coefficient (C_D).

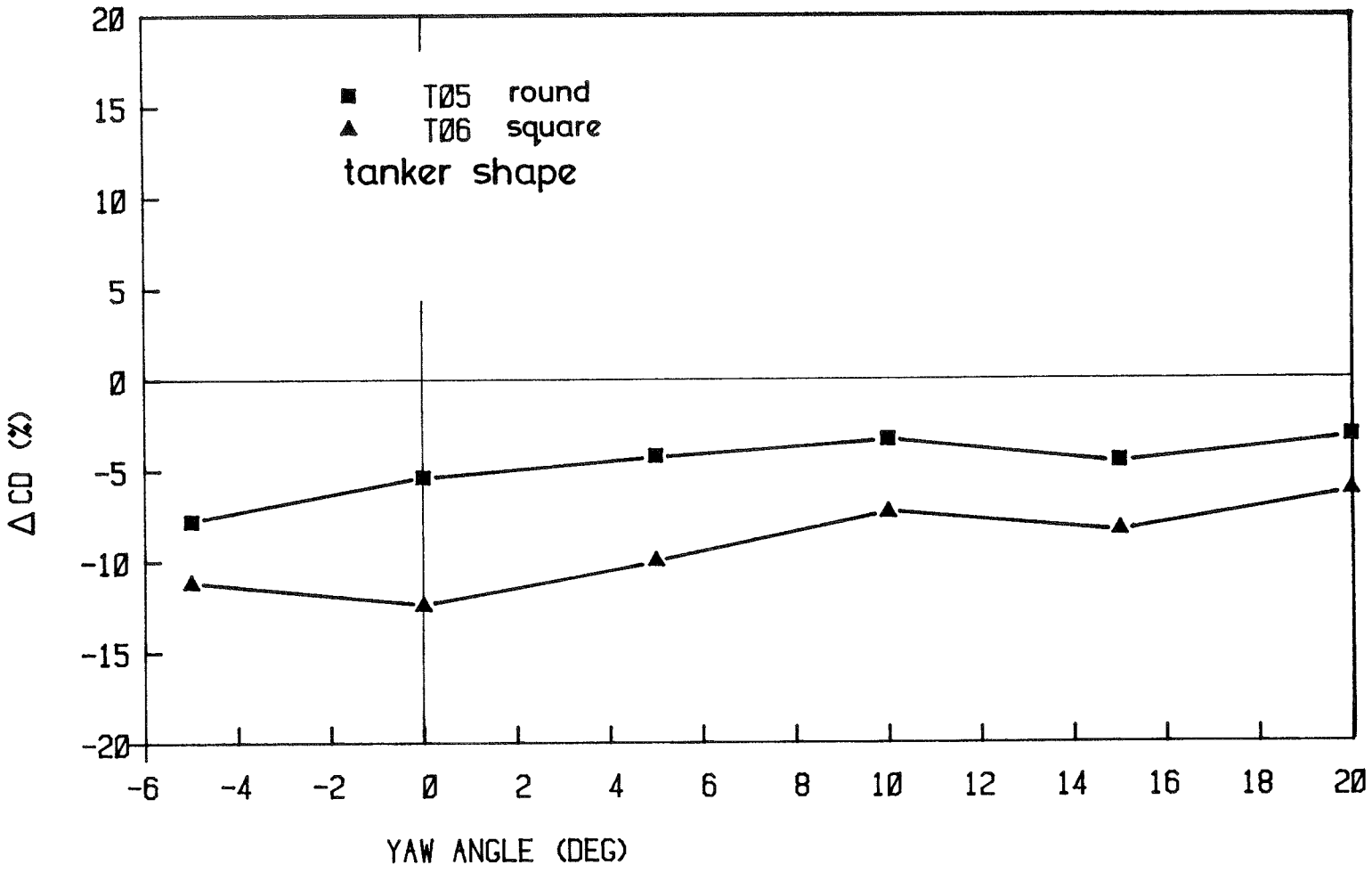

Figure 22. The influence of tanker forebody and end shape on drag coefficient (C_D).

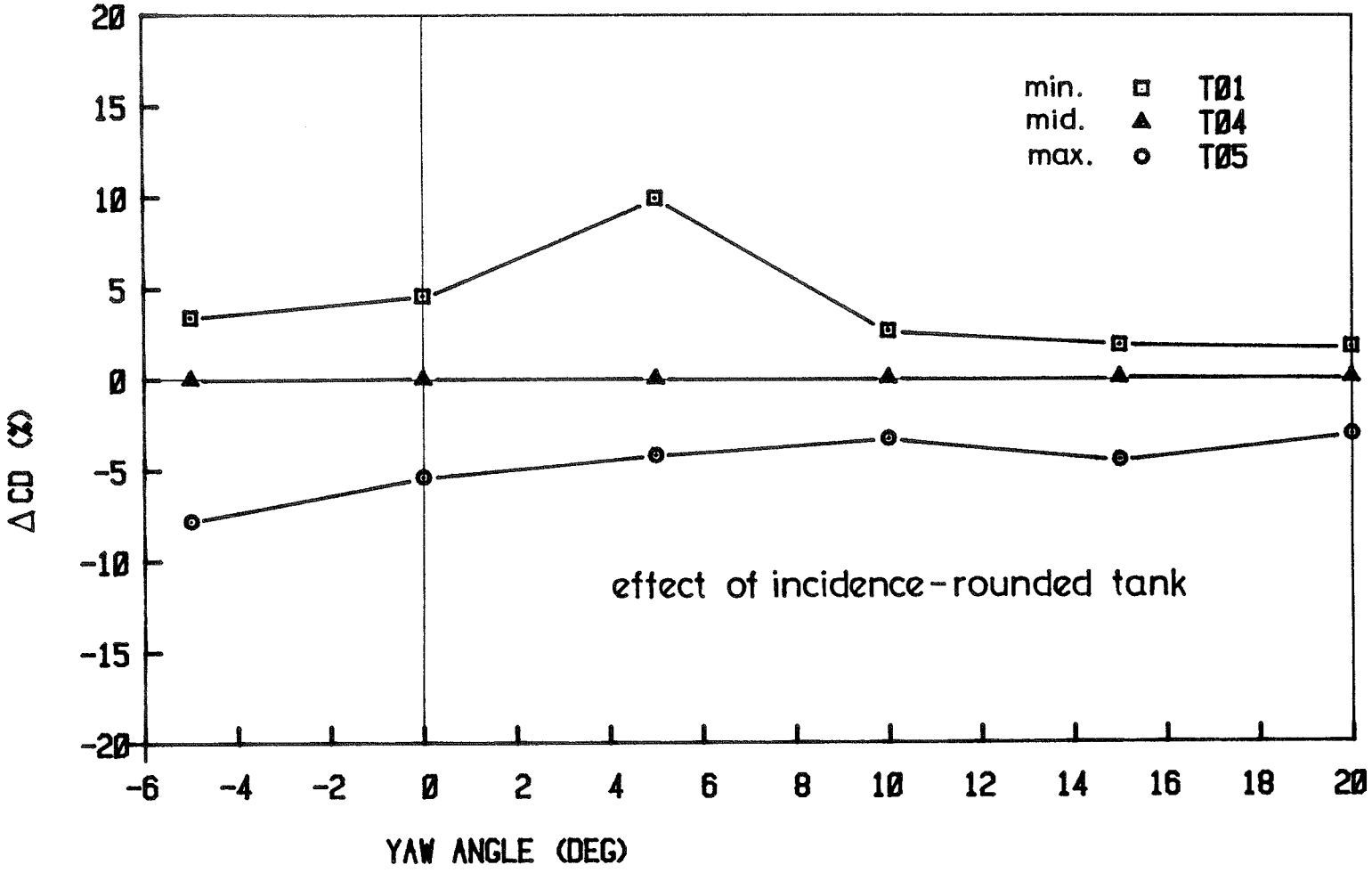

Figure 23. The effect of streamlined tanker incidence on drag coefficient (C_D).

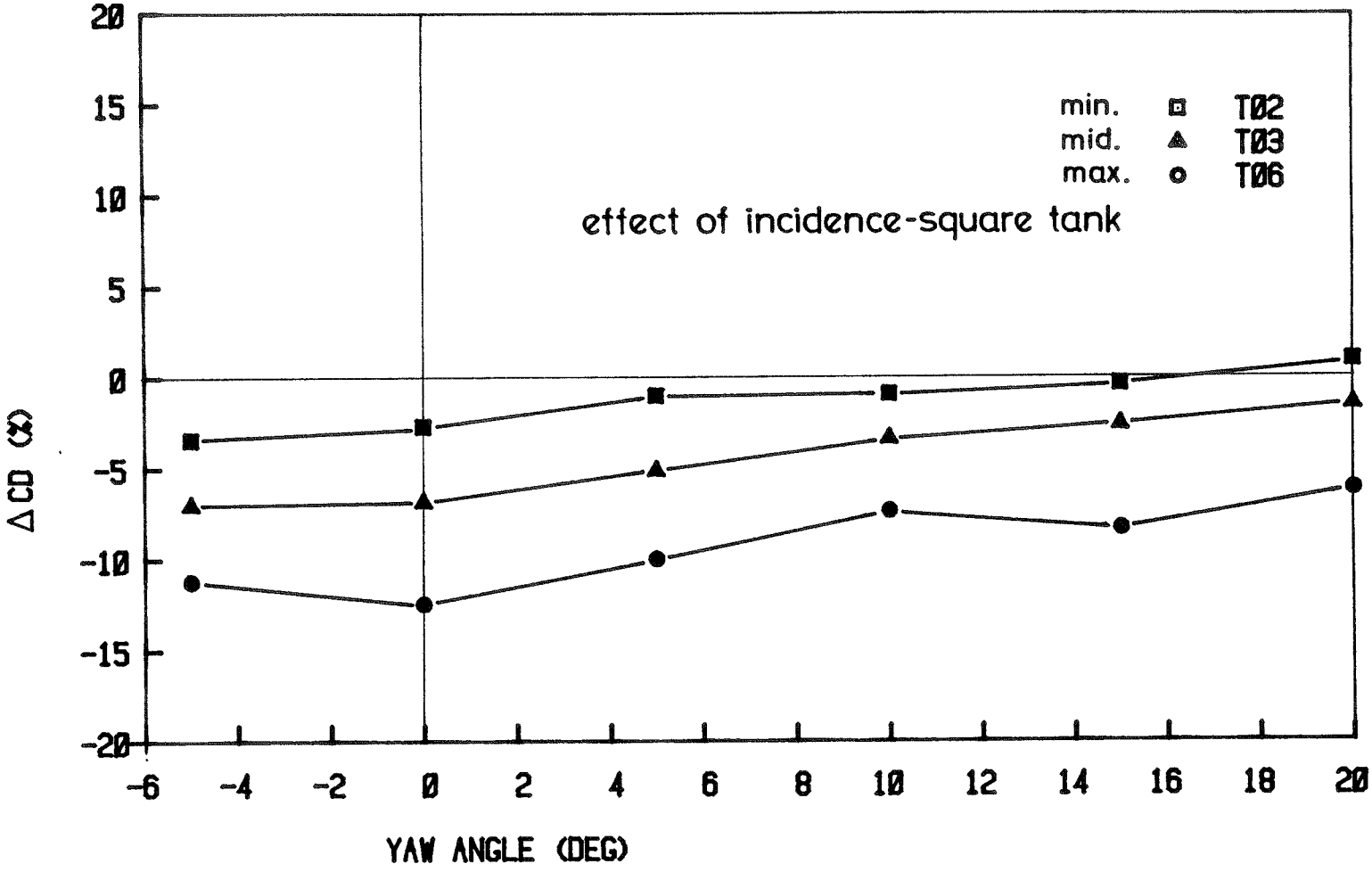

Figure 24. The influence of 'square' tanker incidence on drag coefficient (C_D).

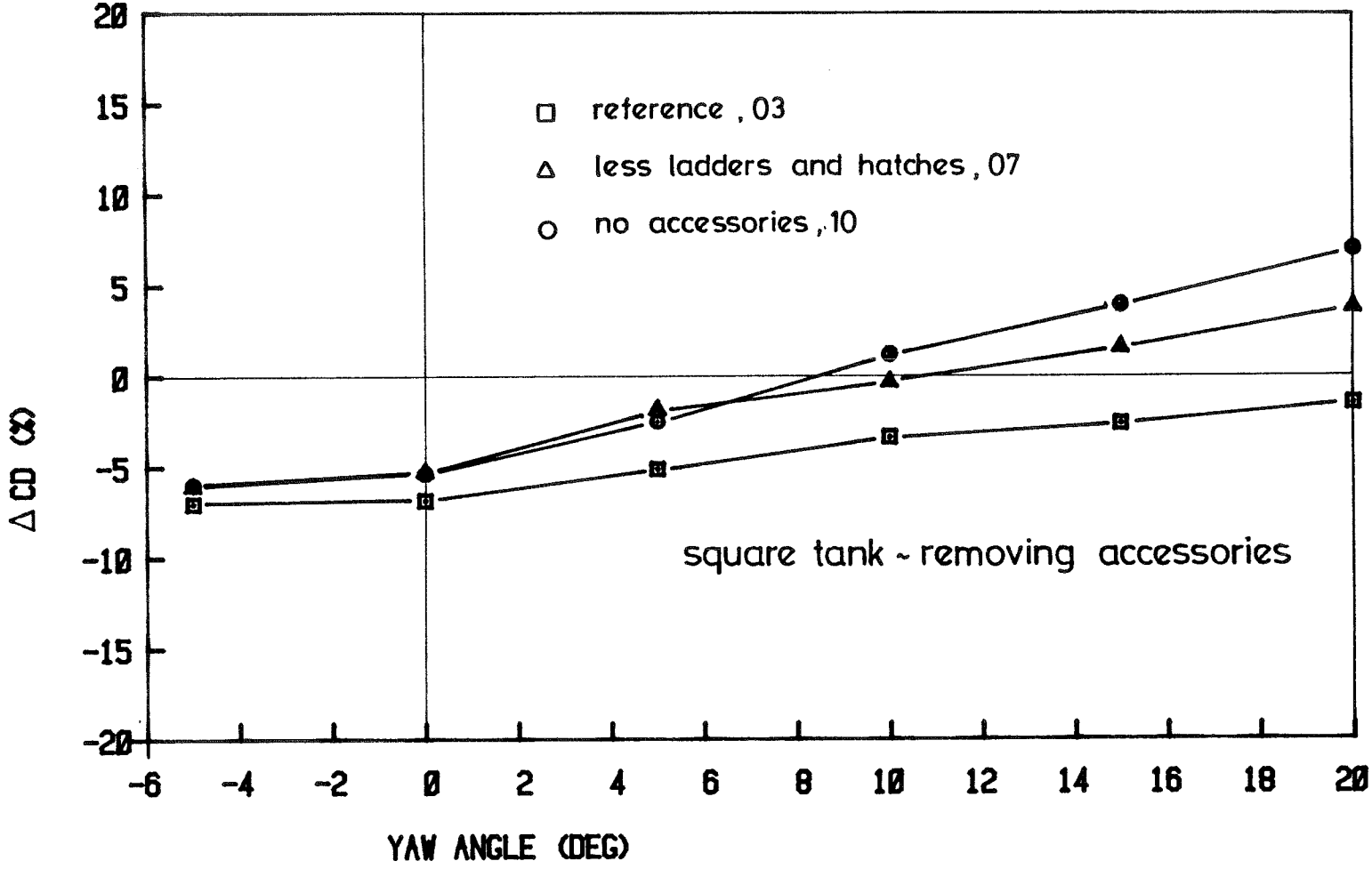

Figure 25. The influence of ancillary components for the square edged tanker on drag coefficient (C_D).

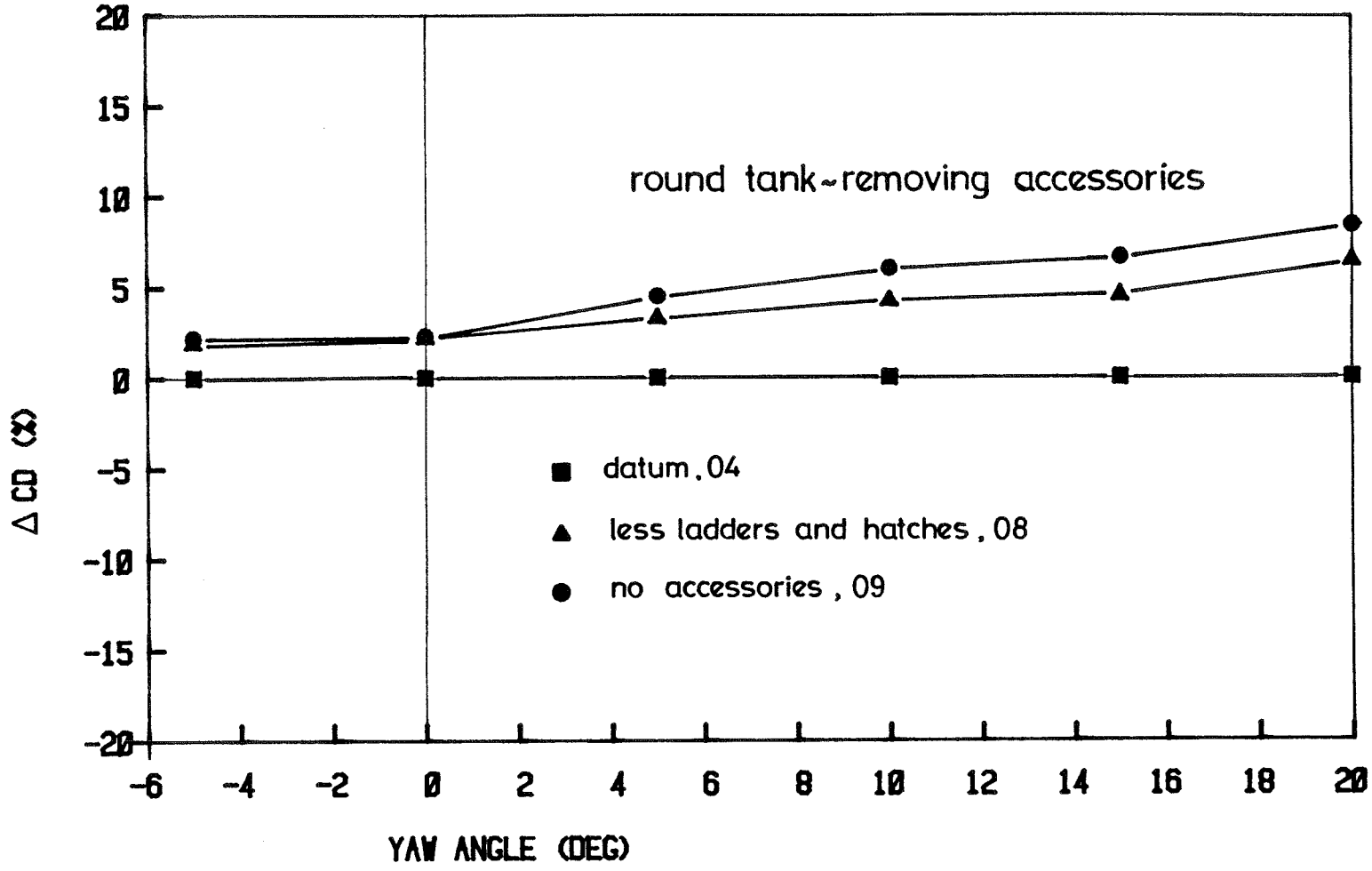

Figure 26. The influence of ancillary components for the streamlined tanker on drag coefficient (C_D).

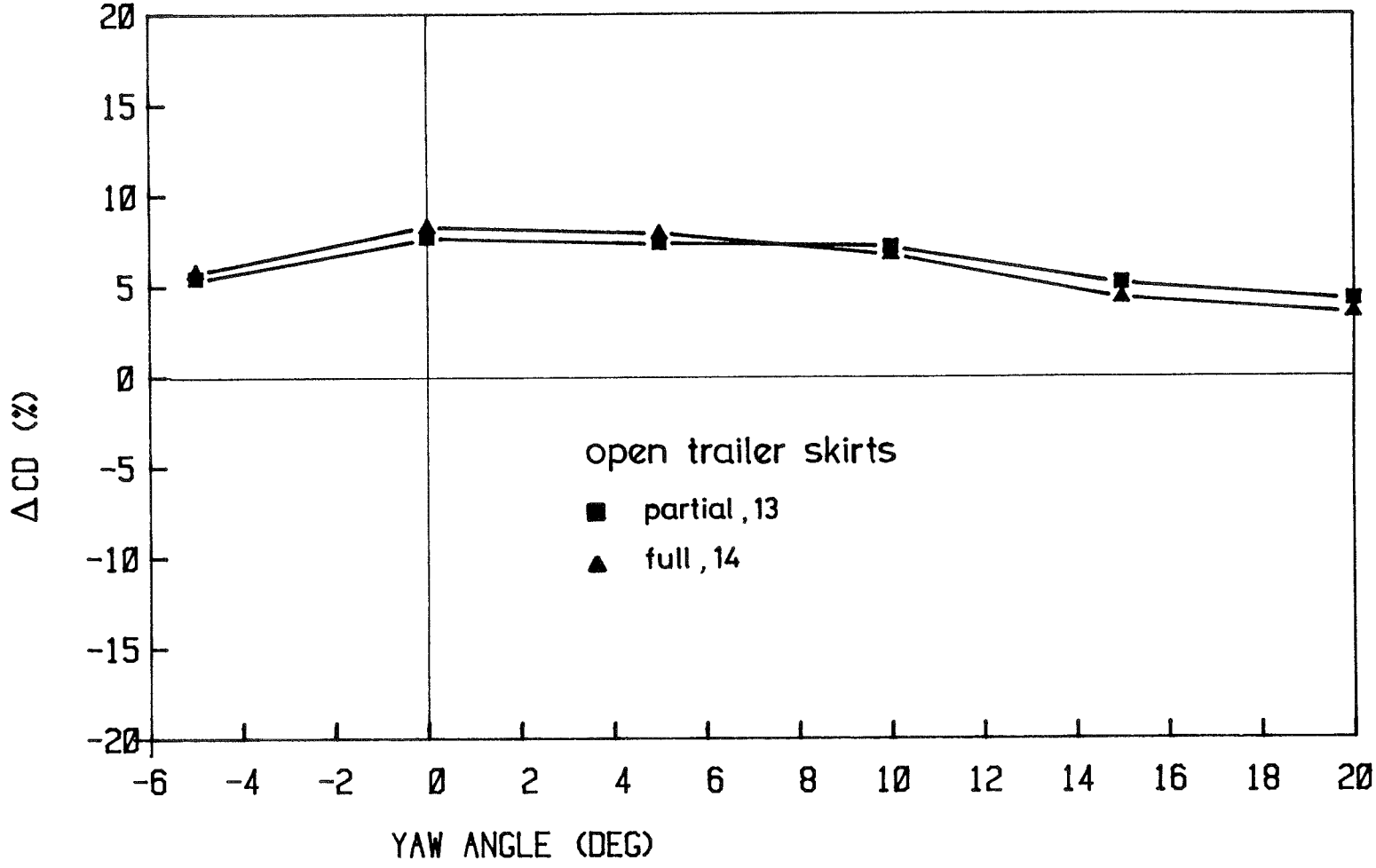

Figure 27. Comparison of partial and full open trailer skirts.

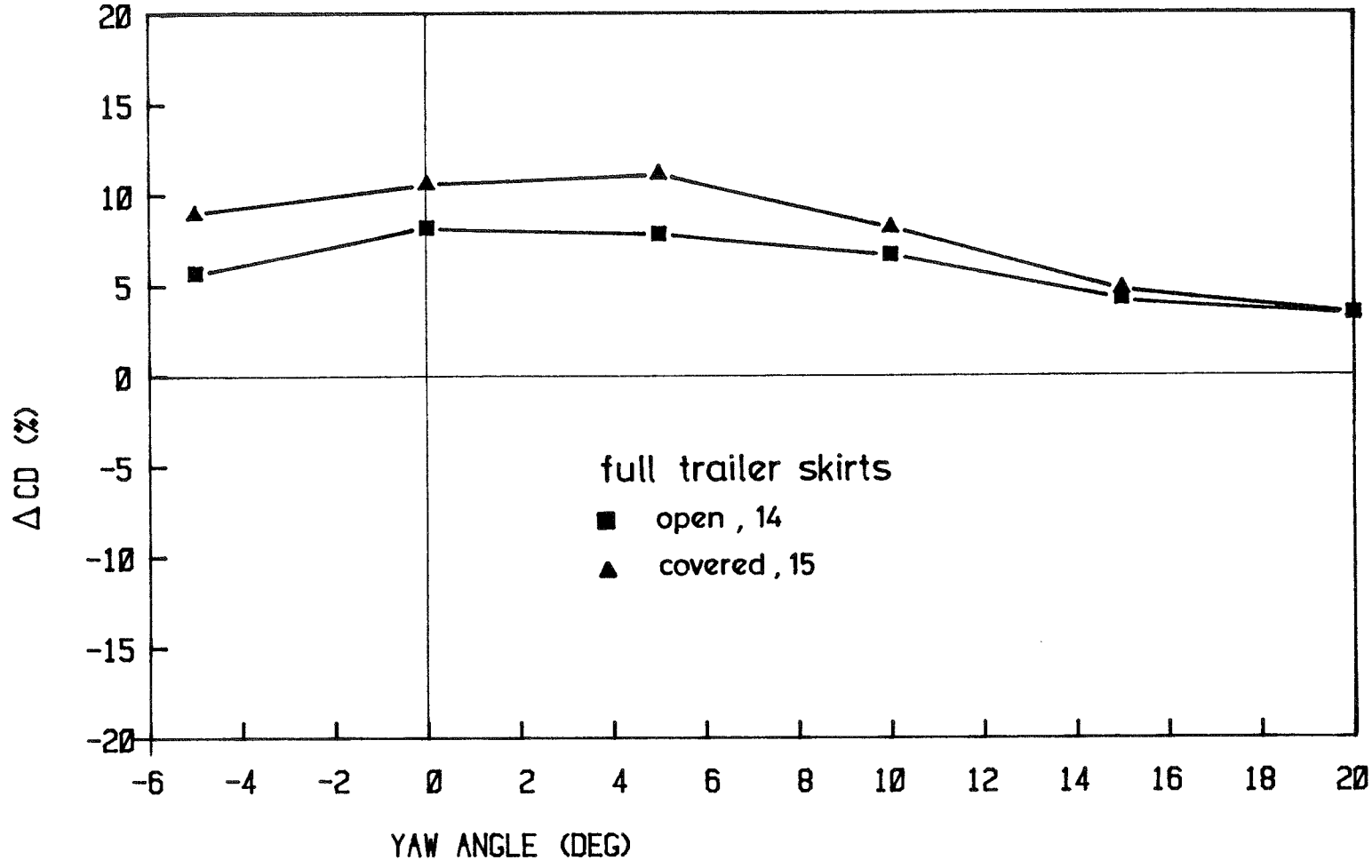

Figure 28. Variation in drag coefficient with open or covered full trailer skirts.

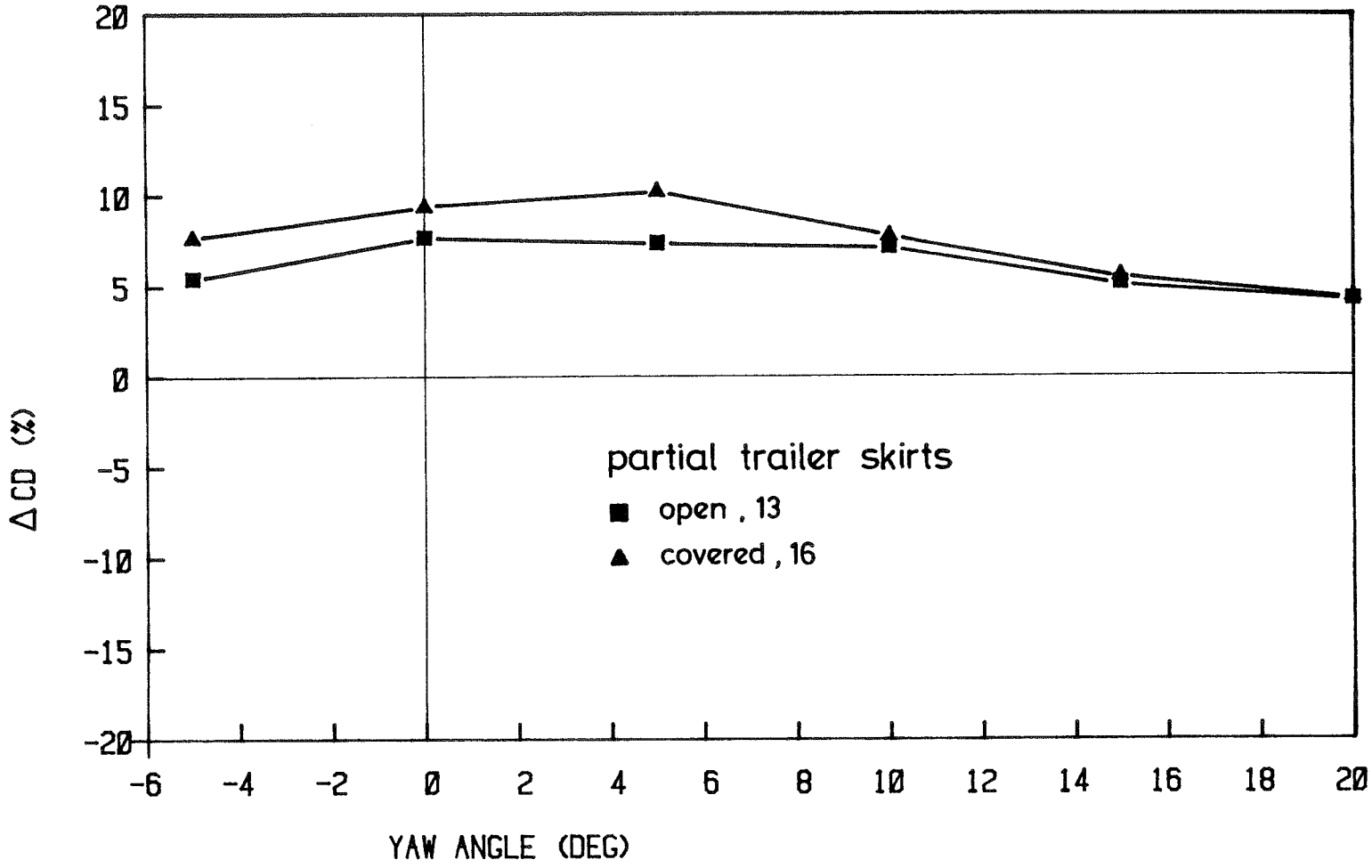

Figure 29. Comparison of open and covered partial trailer skirts.

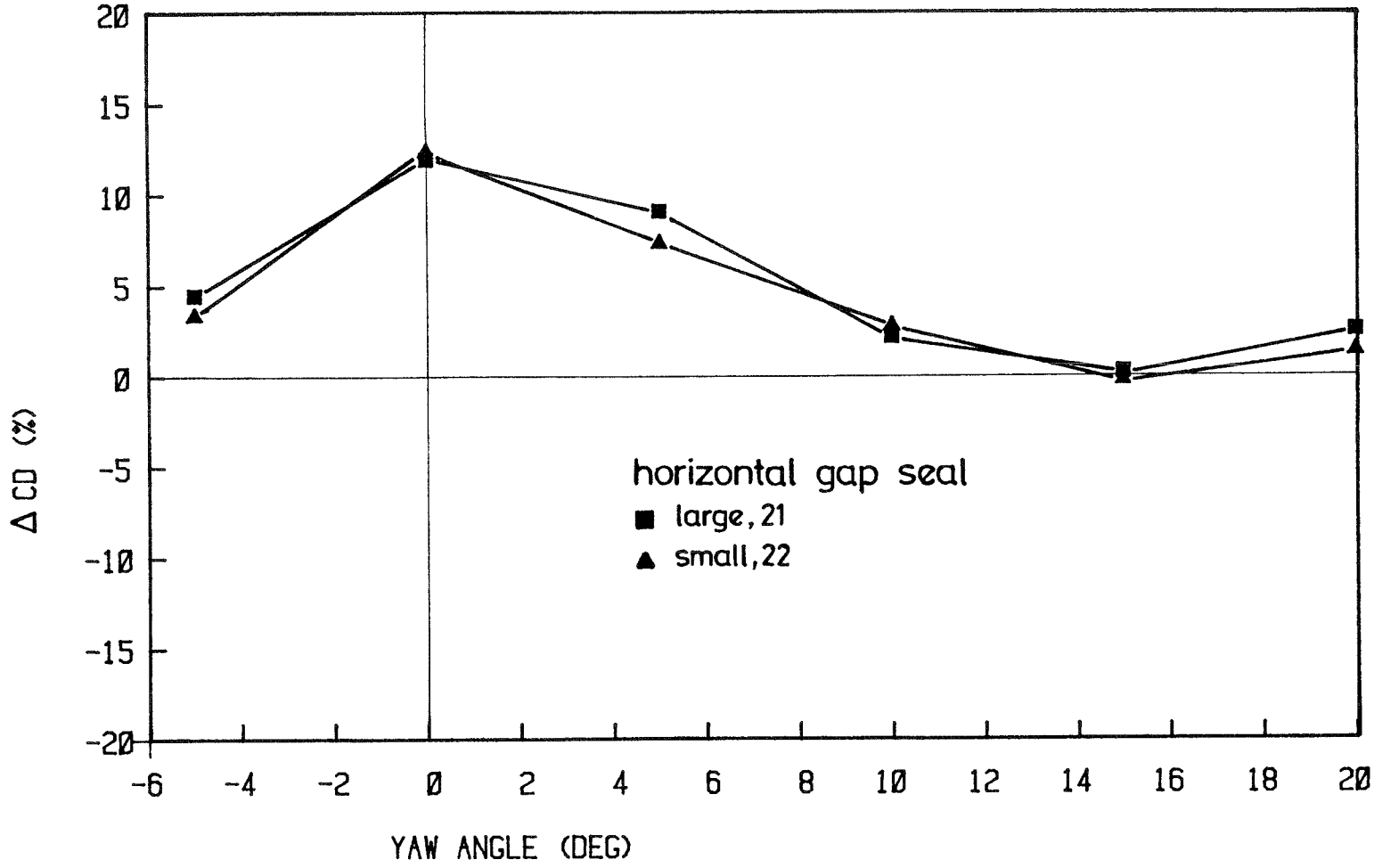

Figure 30. The influence of tractor cab to tanker forebody horizontal gap seals on drag coefficient (C_D)

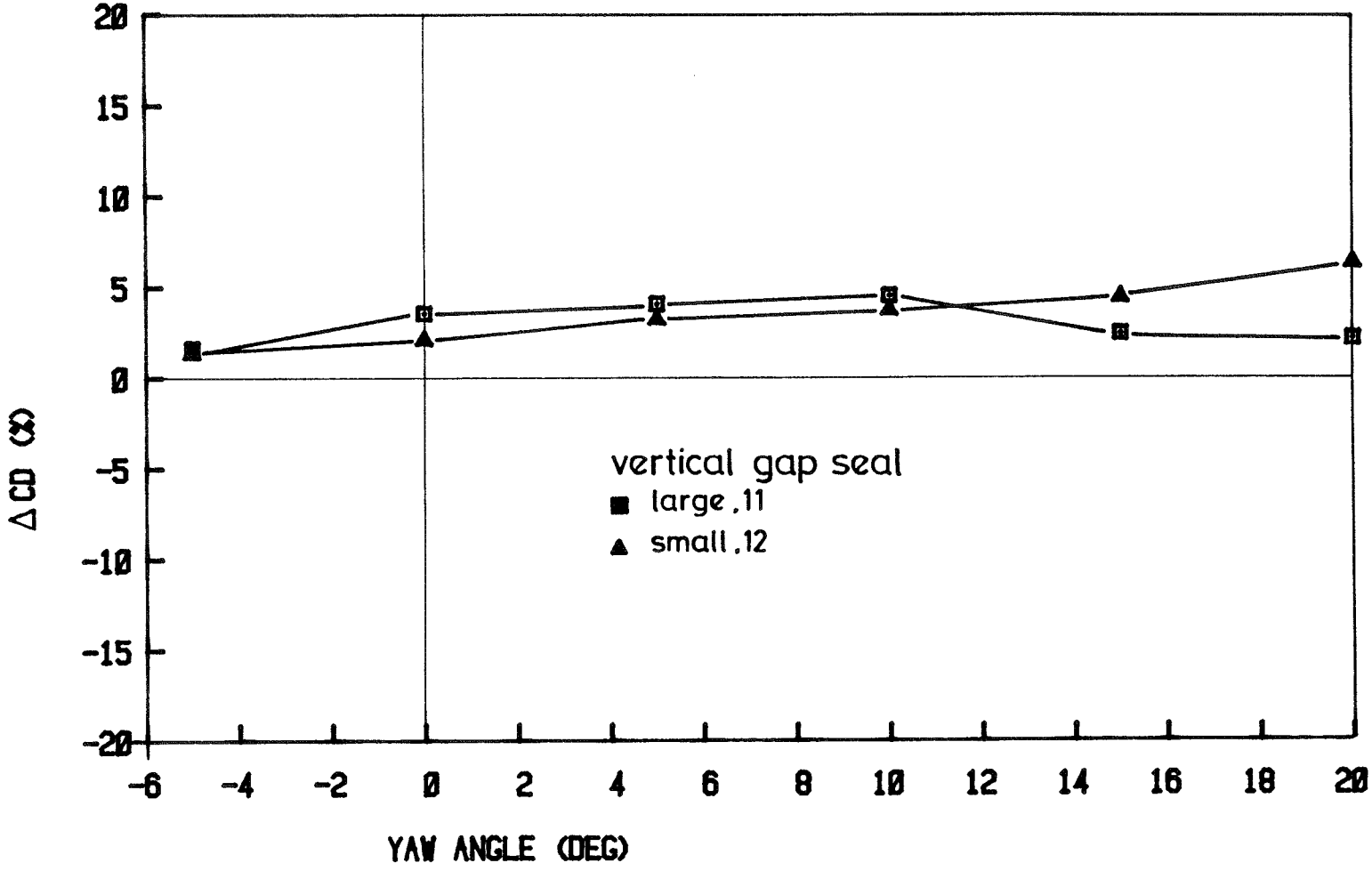

Figure 31. The influence of tractor cab to tanker forebody vertical gap seals on drag coefficient (C_D).

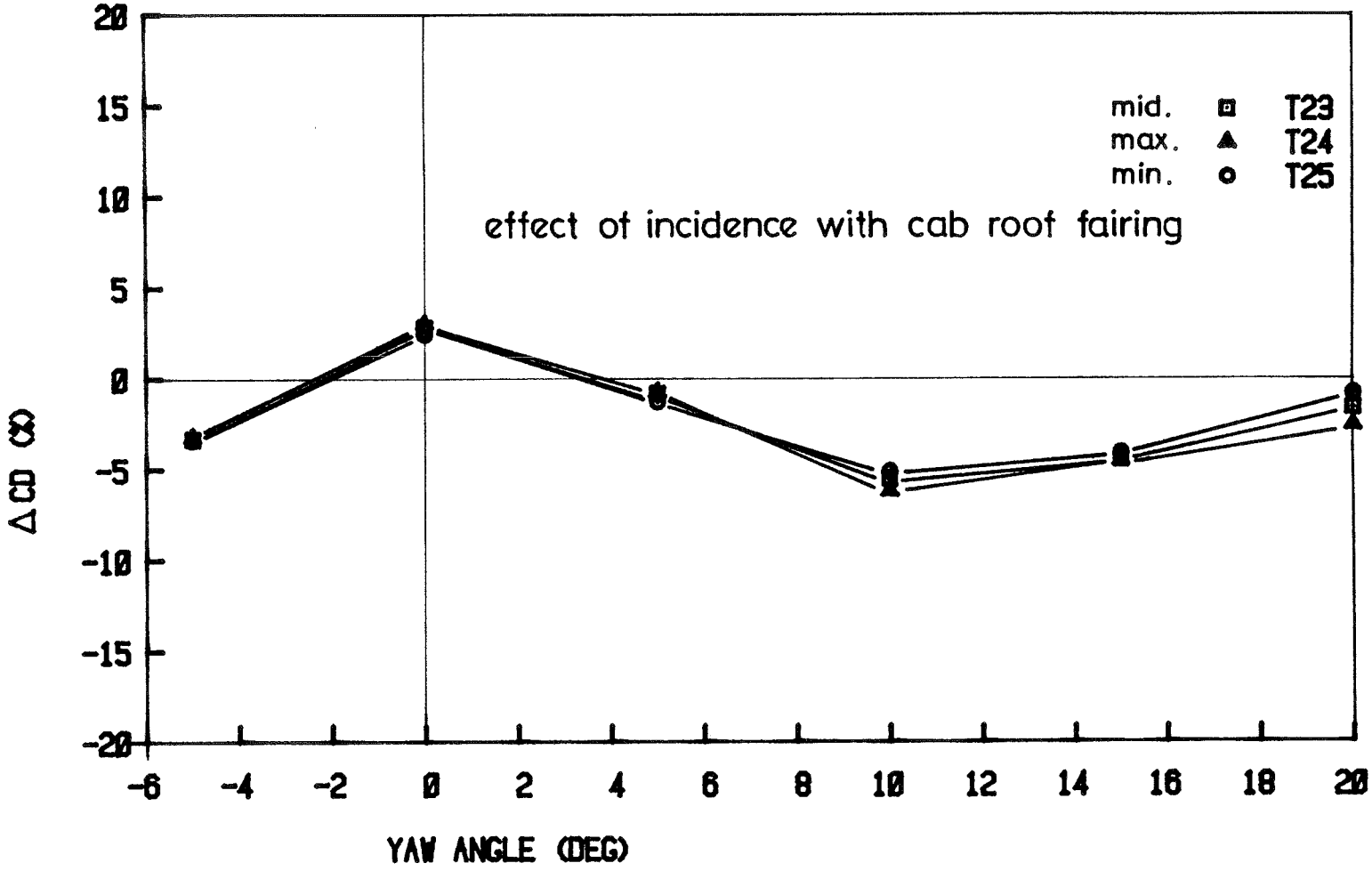

Figure 32. The influence of changes in tanker incidence on drag coefficient for a vehicle fitted with a cab roof fairing.

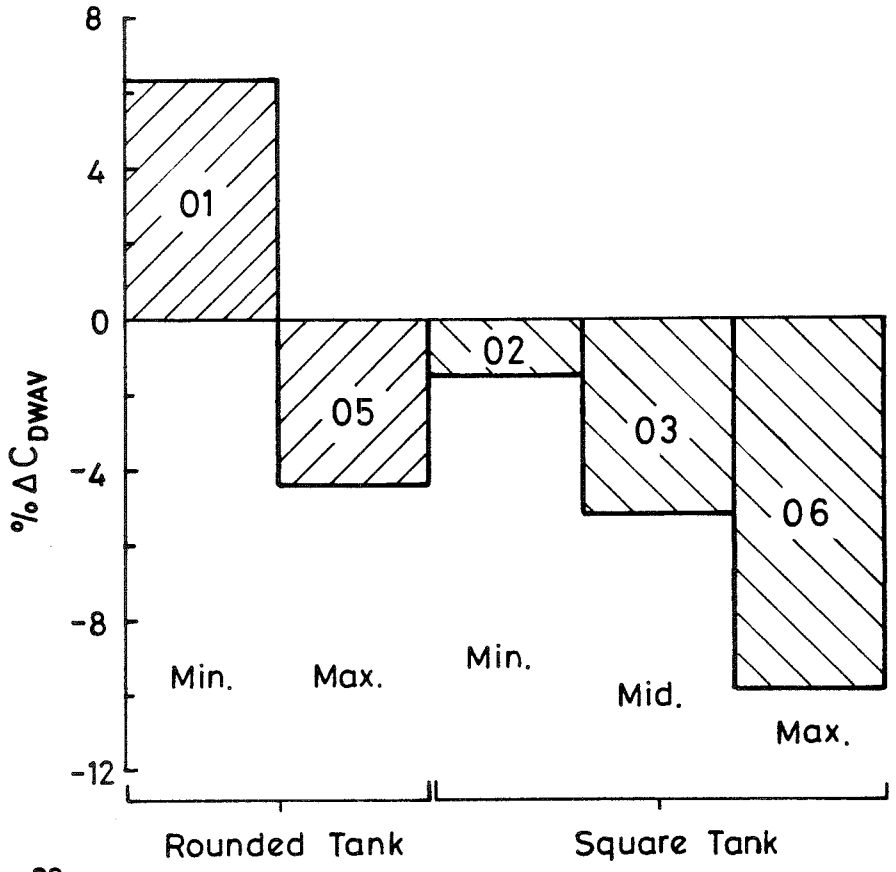

Figure 33.

The effect of tank incidence and geometry on wind averaged drag.

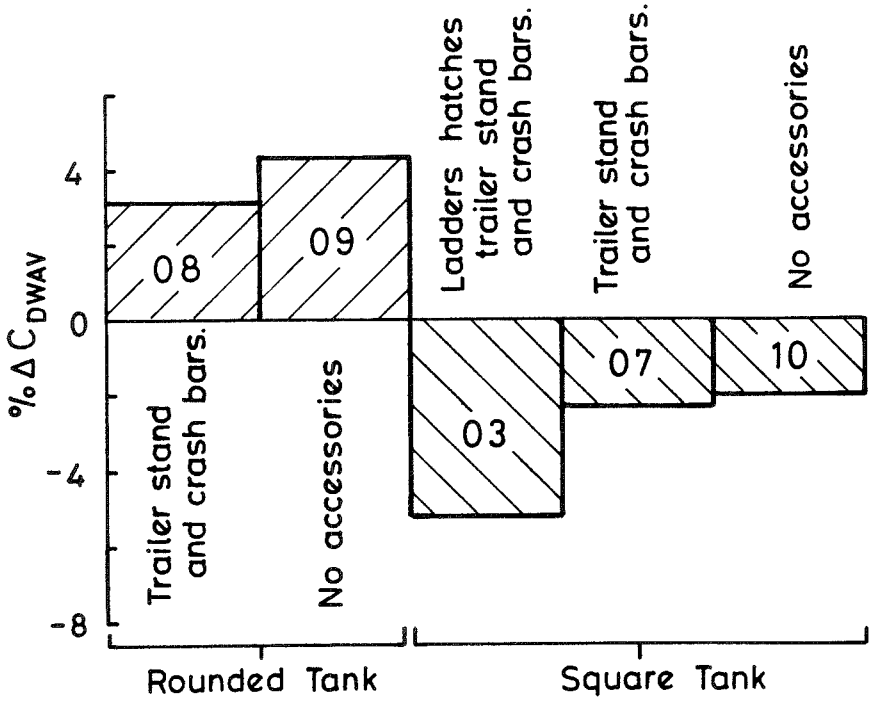

Figure 34.

The effect of tank accessories on wind averaged drag.

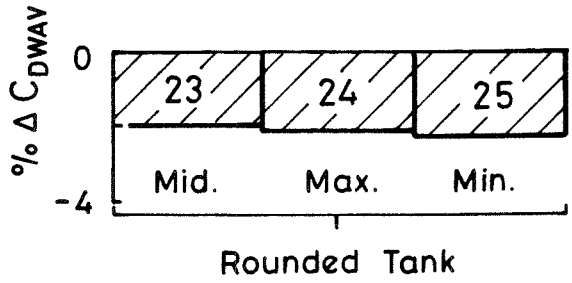

Figure 35.

The influence of tank incidence on wind averaged drag with the standard cab roof fairing.

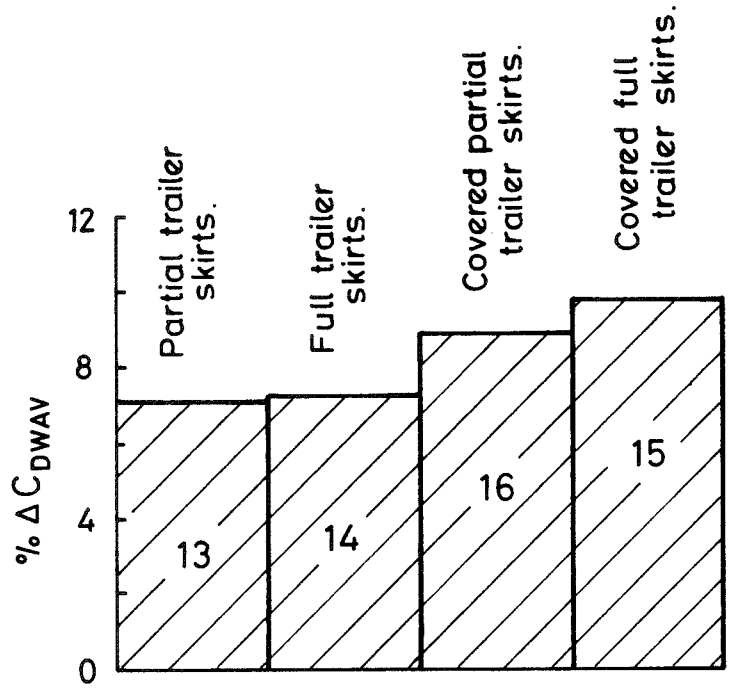

Figure 36.

The influence of skirt geometry on wind averaged drag with a rounded tank.

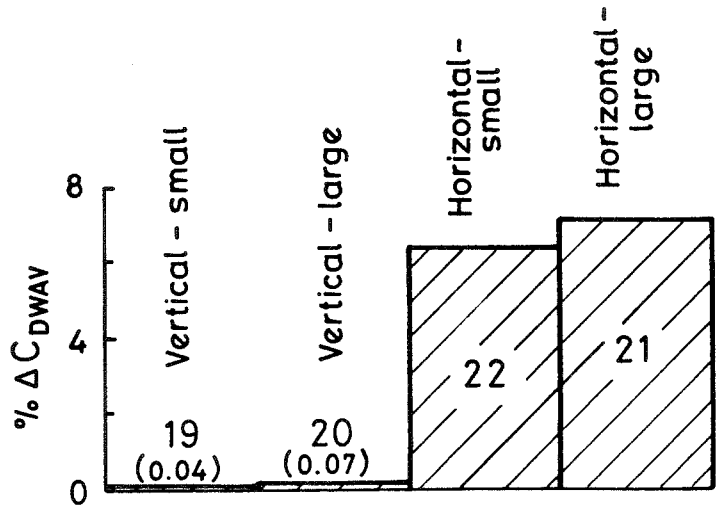

Figure 37.

The effectiveness of tractor trailer gap seals on wind averaged drag for the rounded tanker.

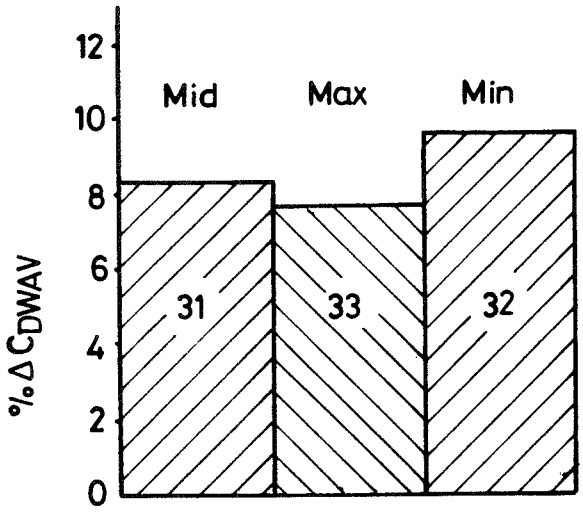

Figure 38
The influence of tank incidence on wind averaged drag for the tanker cab roof fairing.

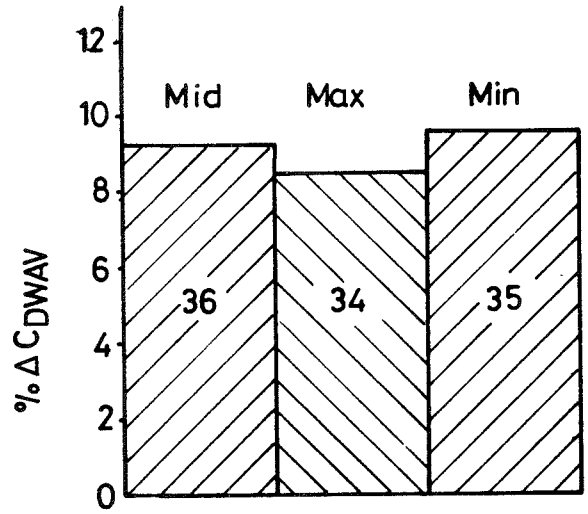

Figure 39.
The influence of tank incidence on wind averaged drag for the tanker cab roof fairing with side extensions.

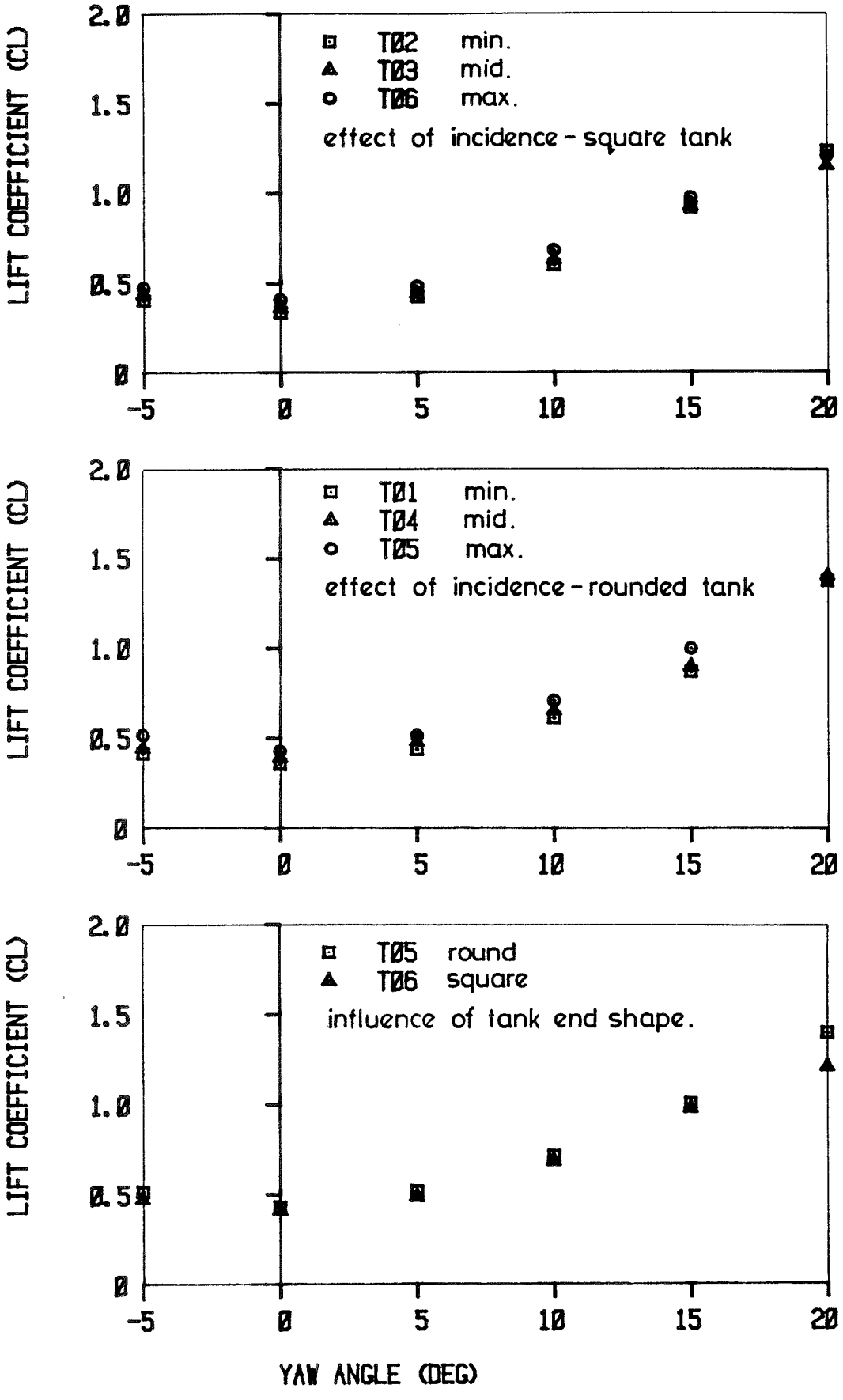

Figure 40. The influence of (a) incidence and (b) tanker end shape on lift coefficient (C_L).

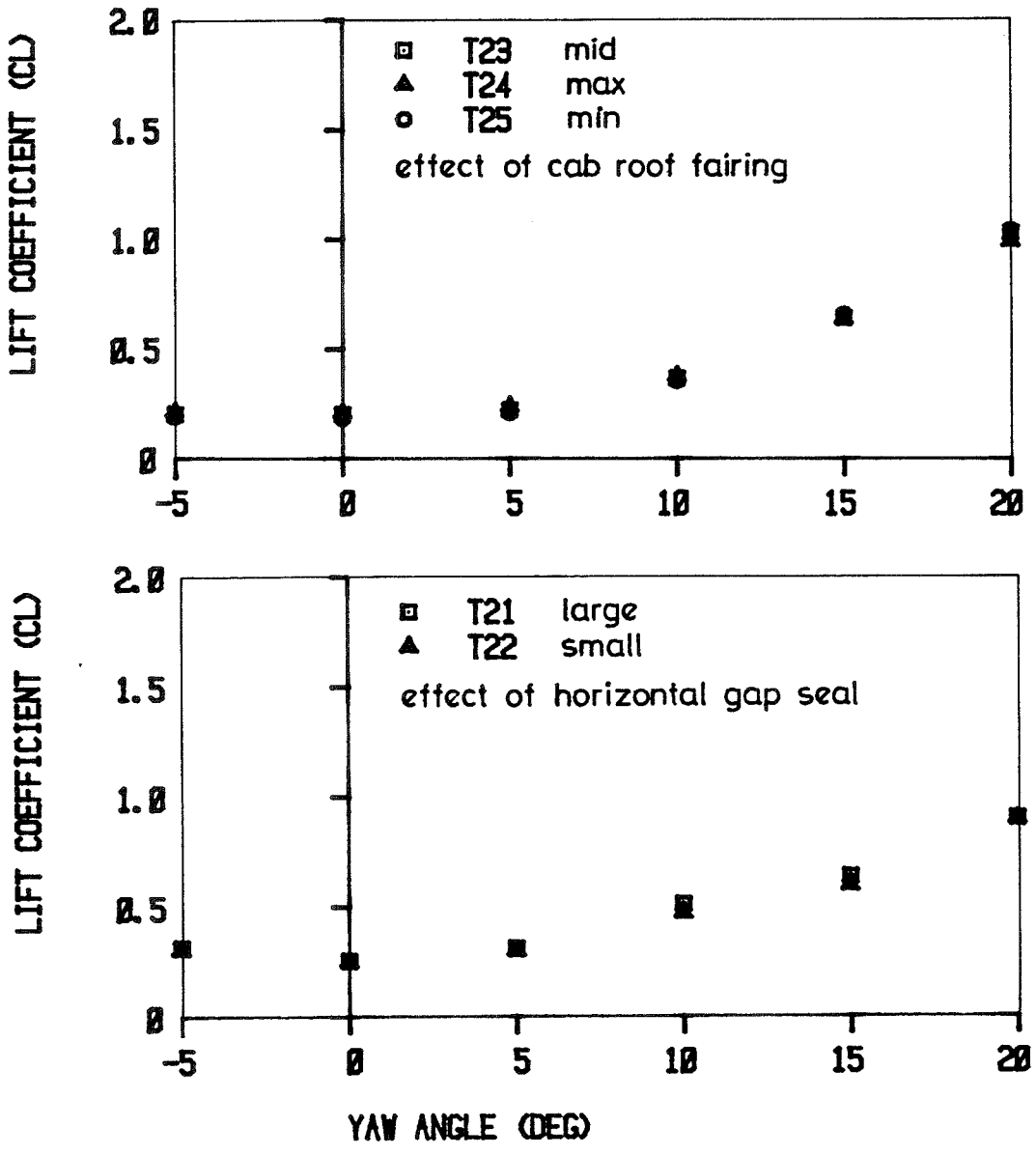

Figure 41. The influence of (a) cab roof mounted fairings and (b) horizontal gap seals on lift coefficient (C_L).

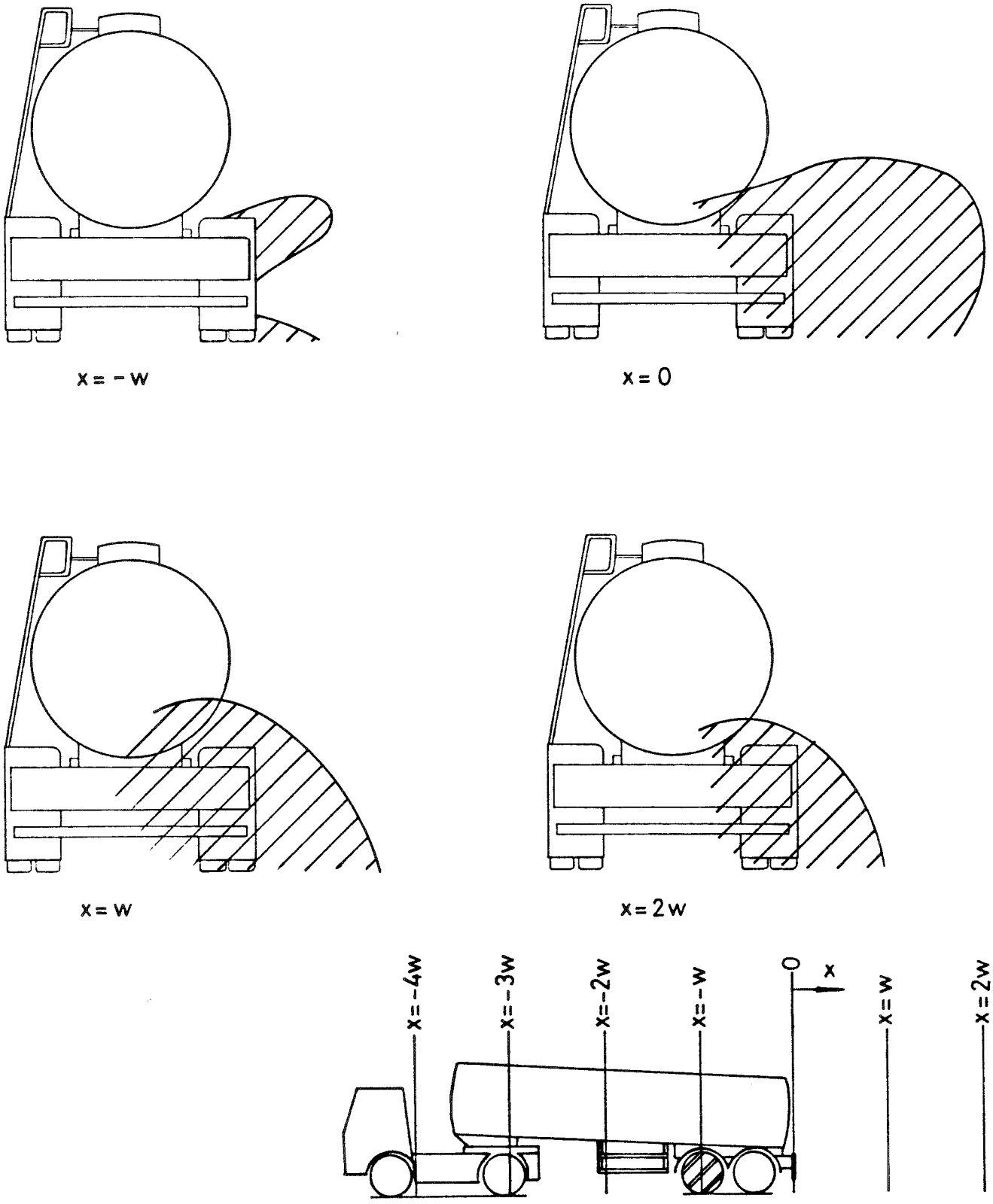

Figure 42. Baseline vehicle wake flow visualisation, smoke source in rear wheelarch.

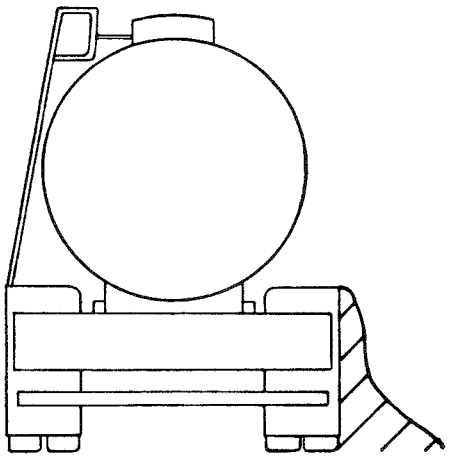

x = -3w

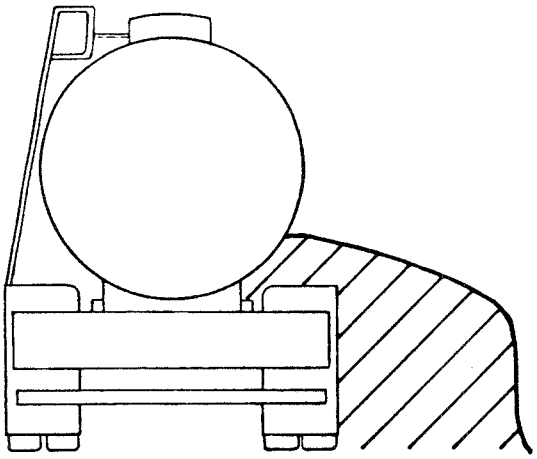

x = -2w

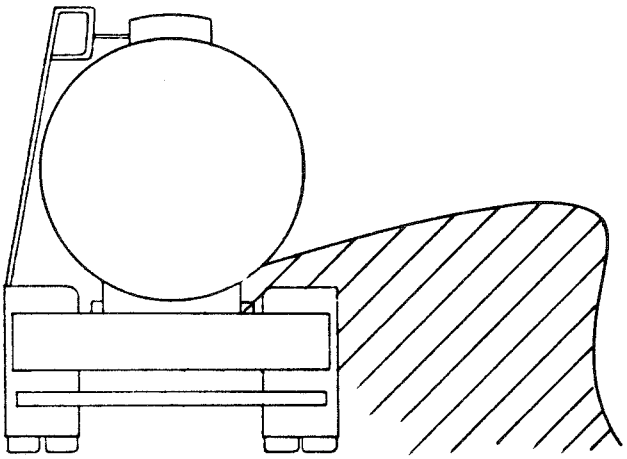

x = -w

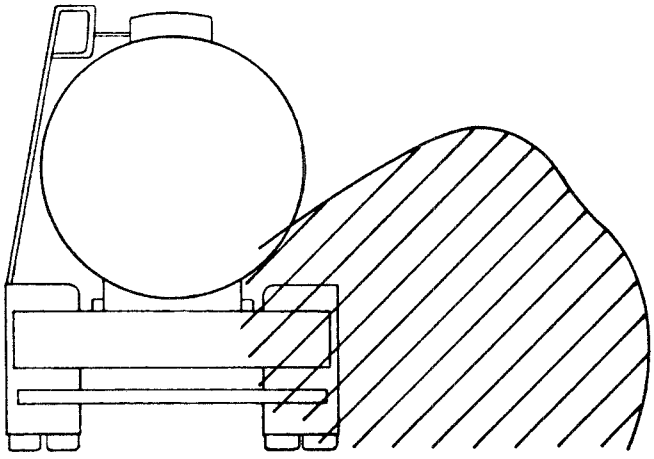

x = 0

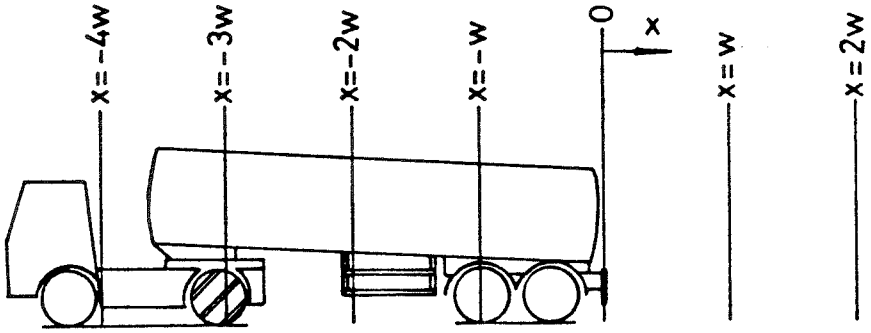

Figure 43(a). Baseline vehicle wake flow visualisation, smoke source in the centre wheelarch.

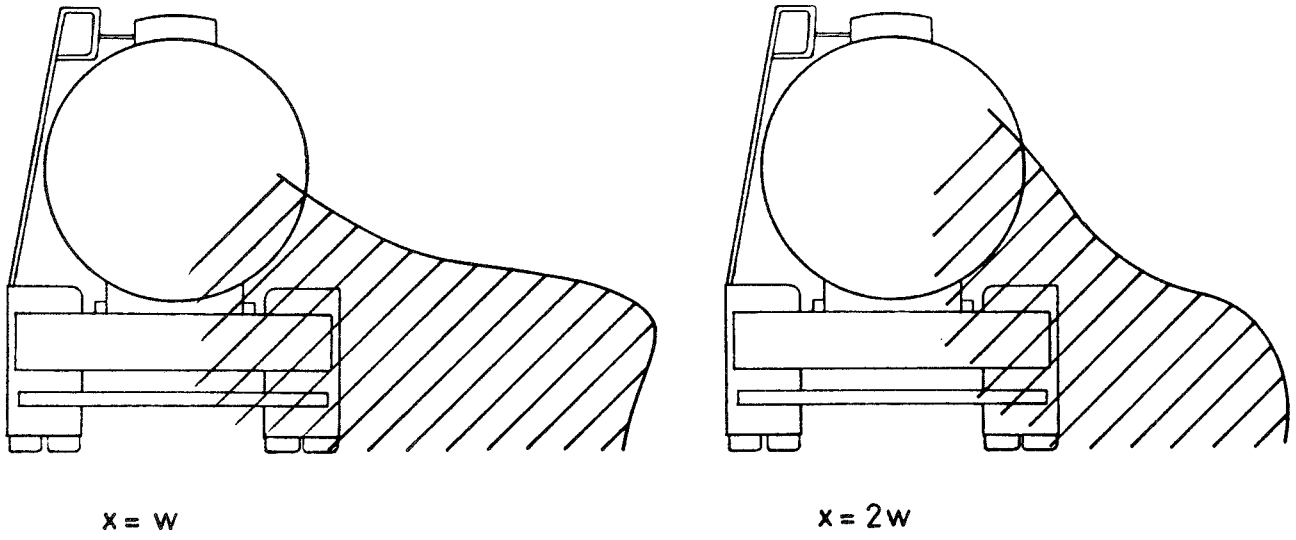

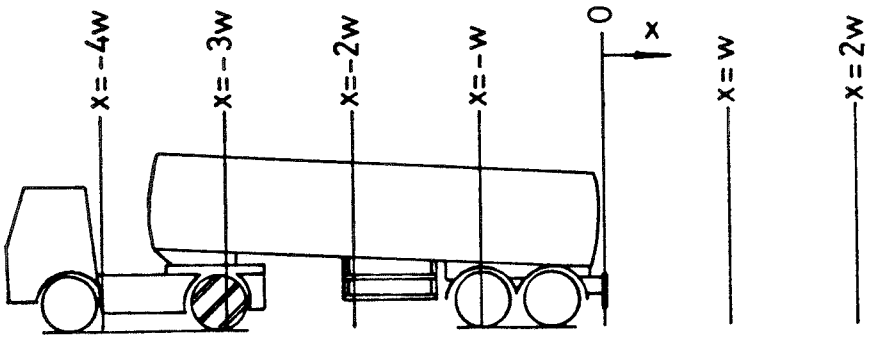

Figure 43(b). Baseline vehicle wake flow visualisation, smoke source in the centre wheelarch.

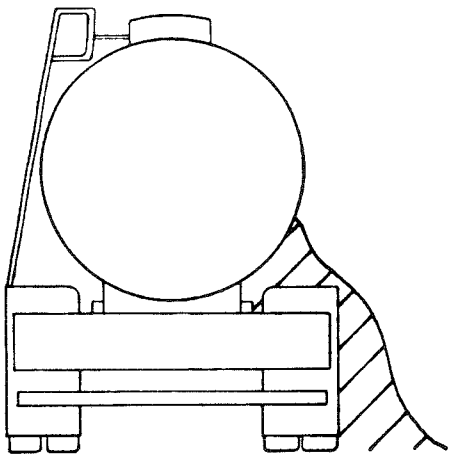

x = -4w

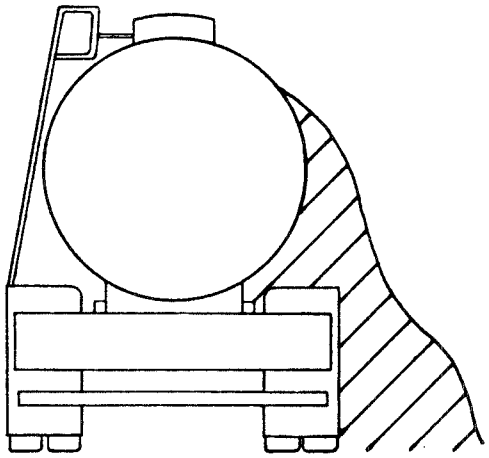

x = -3w

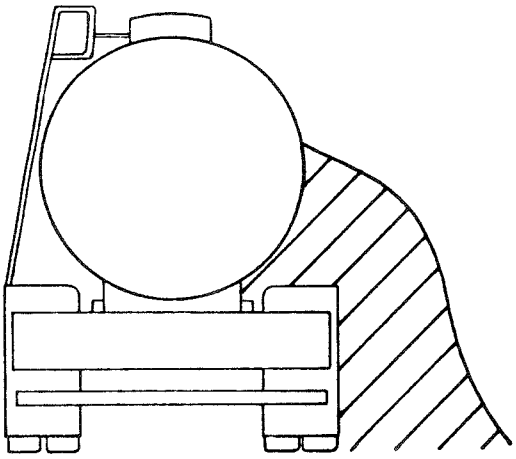

x = -2w

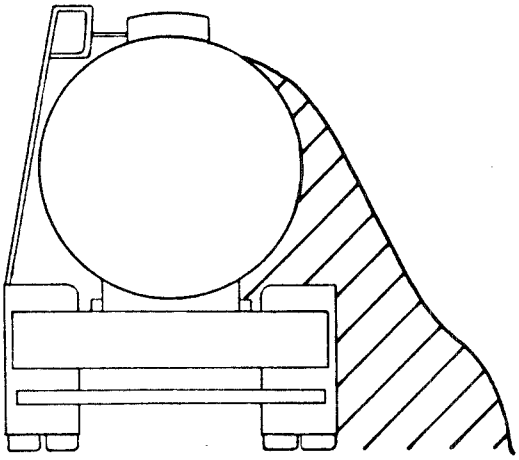

x = -w

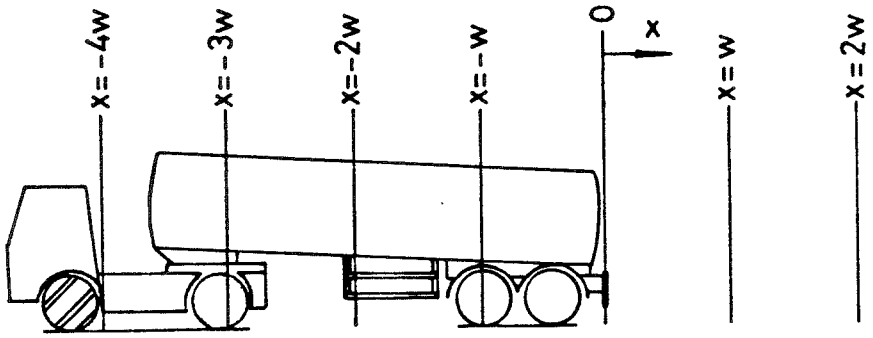

Figure 44(a). Baseline vehicle wake flow visualisation, smoke source in the front wheelarch.

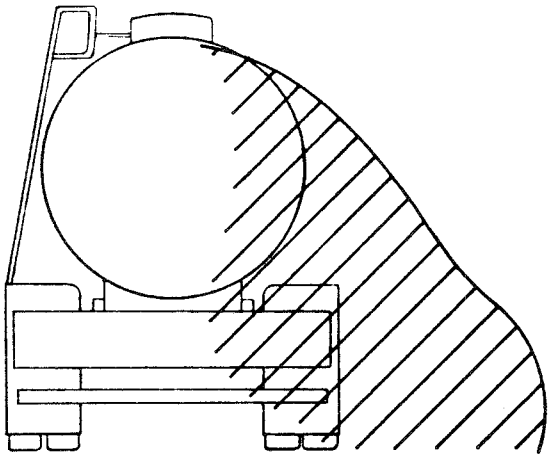

x = 0

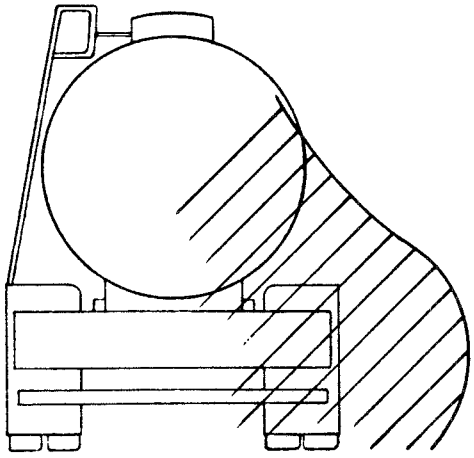

x = w

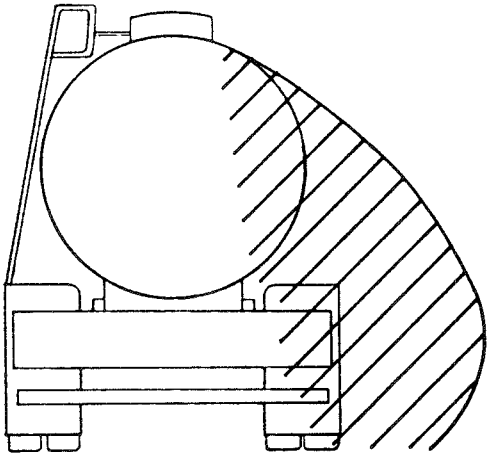

x = 2w

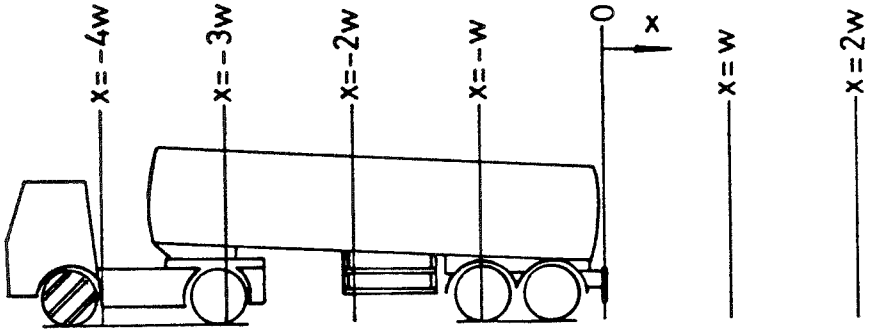

Figure 44(b). Baseline vehicle wake flow visualisation, smoke source in front wheelarch.

APPENDIX A

MODEL CONFIGURATION: T01

YAW ANGLE	LIFT COEF.	DRAG COEF.	SIDE COEF.	PITCH COEF.	ROLL COEF.	YAW COEF.
-5.0	0.415	1.018	0.267	1.446	0.893	0.215
0.0	0.357	0.922	0.031	1.567	0.217	0.030
-5.0	0.439	0.966	-0.428	1.393	-0.022	-0.210
10.0	0.617	1.351	-0.393	1.607	-0.739	-0.230
15.0	0.875	1.798	-0.491	1.436	-1.094	-0.340
20.0	1.380	2.352	-0.662	1.277	-2.012	-0.655

MODEL CONFIGURATION: T02

YAW ANGLE	LIFT COEF.	DRAG COEF.	SIDE COEF.	PITCH COEF.	ROLL COEF.	YAW COEF.
-5.0	0.405	1.090	0.244	1.666	0.839	0.186
0.0	0.338	0.992	0.010	1.762	0.133	0.012
5.0	0.427	1.083	-0.263	1.782	-0.790	-0.237
10.0	0.601	1.401	-0.342	1.795	-0.674	-0.174
15.0	0.919	1.837	-0.424	1.736	-1.004	-0.253
20.0	1.232	2.371	-0.492	1.526	-1.604	-0.455

MODEL CONFIGURATION: T03

YAW ANGLE	LIFT COEF.	DRAG COEF.	SIDE COEF.	PITCH COEF.	ROLL COEF.	YAW COEF.
-5.0	0.437	1.129	0.245	1.716	0.939	0.216
0.0	0.361	1.032	-0.007	1.854	0.142	0.005
5.0	0.440	1.128	-0.255	1.867	-0.790	-0.235
10.0	0.627	1.435	-0.332	1.848	-0.791	-0.199
15.0	0.924	1.879	-0.406	1.728	-1.059	-0.273
20.0	1.151	2.429	-0.484	1.597	-1.579	-0.453

MODEL CONFIGURATION: T04

YAW ANGLE	LIFT COEF.	DRAG COEF.	SIDE COEF.	PITCH COEF.	ROLL COEF.	YAW COEF.
-5.0	0.445	1.055	0.262	1.550	1.069	0.254
0.0	0.391	0.966	0.018	1.670	0.236	0.031
5.0	0.483	1.072	-0.281	1.700	-0.729	-0.243
10.0	0.657	1.388	-0.405	1.689	-0.867	-0.262
15.0	0.904	1.831	-0.498	1.468	-1.183	-0.358
20.0	1.407	2.393	-0.616	1.358	-2.024	-0.635

MODEL CONFIGURATION: T05

YAW ANGLE	LIFT COEF.	DRAG COEF.	SIDE COEF.	PITCH COEF.	ROLL COEF.	YAW COEF.
-5.0	0.517	1.136	0.320	1.784	0.926	0.274
0.0	0.430	1.018	0.042	1.807	0.282	0.058
5.0	0.518	1.117	-0.222	1.821	-0.647	-0.200
10.0	0.712	1.434	-0.447	1.670	-1.212	-0.354
15.0	1.005	1.913	-0.582	1.553	-1.603	-0.487
20.0	1.395	2.467	-0.629	1.360	-2.212	-0.672

MODEL CONFIGURATION: T06

YAW ANGLE	LIFT COEF.	DRAG COEF.	SIDE COEF.	PITCH COEF.	ROLL COEF.	YAW COEF.
-5.0	0.476	1.173	0.228	1.828	0.939	0.223
0.0	0.410	1.086	0.054	1.956	0.373	0.085
5.0	0.485	1.179	-0.175	1.994	-0.458	-0.126
10.0	0.684	1.490	-0.366	1.885	-0.981	-0.264
15.0	0.975	1.983	-0.431	1.832	-1.201	-0.330
20.0	1.206	2.540	-0.502	1.636	-1.791	-0.516

MODEL CONFIGURATION: T07

YAW ANGLE	LIFT COEF.	DRAG COEF.	SIDE COEF.	PITCH COEF.	ROLL COEF.	YAW COEF.
-5.0	0.467	1.118	0.252	1.703	1.048	0.240
0.0	0.374	1.017	0.068	1.847	0.418	0.097
5.0	0.442	1.092	-0.178	1.822	-0.506	-0.140
10.0	0.652	1.393	-0.325	1.743	-0.913	-0.233
15.0	0.949	1.803	-0.335	1.536	-1.217	-0.292
20.0	1.140	2.304	-0.401	1.373	-1.924	-0.517

MODEL CONFIGURATION: T08

YAW ANGLE	LIFT COEF.	DRAG COEF.	SIDE COEF.	PITCH COEF.	ROLL COEF.	YAW COEF.
-5.0	0.452	1.034	0.270	1.530	1.062	0.252
0.0	0.374	0.945	0.060	1.674	0.285	0.065
5.0	0.459	1.037	-0.202	1.683	-0.564	-0.172
10.0	0.648	1.329	-0.388	1.518	-1.144	-0.320
15.0	0.893	1.749	-0.432	1.296	-1.453	-0.411
20.0	1.323	2.241	-0.458	1.097	-2.114	-0.606

MODEL CONFIGURATION: T09

YAW ANGLE	LIFT COEF.	DRAG COEF.	SIDE COEF.	PITCH COEF.	ROLL COEF.	YAW COEF.
-5.0	0.463	1.031	0.263	1.504	0.875	0.205
0.0	0.390	0.944	0.058	1.620	0.225	0.047
5.0	0.468	1.024	-0.196	1.615	-0.486	-0.157
10.0	0.675	1.305	-0.385	1.455	-1.060	-0.308
15.0	0.944	1.710	-0.441	1.207	-1.359	-0.397
20.0	1.410	2.193	-0.482	1.063	-1.834	-0.565

MODEL CONFIGURATION: T10

YAW ANGLE	LIFT COEF.	DRAG COEF.	SIDE COEF.	PITCH COEF.	ROLL COEF.	YAW COEF.
-5.0	0.471	1.118	0.228	1.697	0.834	0.183
0.0	0.385	1.018	0.011	1.808	0.106	0.011
5.0	0.472	1.099	-0.214	1.799	-0.679	-0.191
10.0	0.681	1.372	-0.276	1.748	-0.691	-0.157
15.0	1.001	1.759	-0.283	1.596	-0.897	-0.196
20.0	1.253	2.226	-0.368	1.339	-1.527	-0.399

MODEL CONFIGURATION: T11

YAW ANGLE	LIFT COEF.	DRAG COEF.	SIDE COEF.	PITCH COEF.	ROLL COEF.	YAW COEF.
-5.0	0.395	1.038	0.435	1.486	1.229	0.377
0.0	0.358	0.932	0.138	1.602	-0.038	0.053
5.0	0.418	1.029	-0.274	1.577	-1.070	-0.287
10.0	0.554	1.326	-0.562	1.420	-1.333	-0.435
15.0	0.750	1.786	-0.708	1.162	-1.932	-0.621
20.0	0.933	2.343	-0.905	0.770	-2.975	-0.990

MODEL CONFIGURATION: T12

YAW ANGLE	LIFT COEF.	DRAG COEF.	SIDE COEF.	PITCH COEF.	ROLL COEF.	YAW COEF.
-5.0	0.438	1.040	0.320	1.544	1.166	0.301
0.0	0.380	0.946	0.036	1.676	0.204	0.037
5.0	0.445	1.038	-0.284	1.665	-0.912	-0.284
10.0	0.589	1.336	-0.419	1.641	-1.077	-0.316
15.0	0.795	1.750	-0.531	1.314	-1.686	-0.502
20.0	1.090	2.244	-0.644	0.981	-2.431	-0.760

MODEL CONFIGURATION: T13

YAW ANGLE	LIFT COEF.	DRAG COEF.	SIDE COEF.	PITCH COEF.	ROLL COEF.	YAW COEF.
-5.0	0.504	0.997	0.368	1.480	0.904	0.312
0.0	0.422	0.892	0.033	1.584	-0.044	0.040
5.0	0.511	0.993	-0.345	1.551	-1.194	-0.296
10.0	0.728	1.288	-0.601	1.384	-1.804	-0.483
15.0	0.936	1.735	-0.763	0.992	-2.620	-0.722
20.0	1.434	2.290	-0.909	0.671	-3.582	-1.027

MODEL CONFIGURATION: T14

YAW ANGLE	LIFT COEF.	DRAG COEF.	SIDE COEF.	PITCH COEF.	ROLL COEF.	YAW COEF.
-5.0	0.518	0.994	0.366	1.497	0.815	0.279
0.0	0.430	0.887	0.015	1.577	-0.065	0.026
5.0	0.543	0.988	-0.347	1.565	-0.984	-0.245
10.0	0.740	1.295	-0.625	1.405	-1.771	-0.472
15.0	0.966	1.751	-0.805	1.065	-2.580	-0.716
20.0	1.424	2.310	-0.940	0.776	-3.496	-1.000

MODEL CONFIGURATION: T15

YAW ANGLE	LIFT COEF.	DRAG COEF.	SIDE COEF.	PITCH COEF.	ROLL COEF.	YAW COEF.
-5.0	0.467	0.960	0.412	1.470	0.914	0.314
0.0	0.393	0.864	0.058	1.561	-0.046	0.047
5.0	0.478	0.953	-0.336	1.552	-0.999	-0.236
10.0	0.697	1.274	-0.672	1.363	-1.806	-0.487
15.0	0.954	1.743	-0.883	0.967	-2.751	-0.776
20.0	1.441	2.310	-1.002	0.559	-3.750	-1.078

MODEL CONFIGURATION: T16

YAW ANGLE	LIFT COEF.	DRAG COEF.	SIDE COEF.	PITCH COEF.	ROLL COEF.	YAW COEF.
-5.0	0.471	0.974	0.390	1.459	0.919	0.315
0.0	0.369	0.875	0.047	1.582	-0.050	0.044
5.0	0.468	0.963	-0.324	1.569	-1.016	-0.240
10.0	0.702	1.281	-0.677	1.391	-1.881	-0.525
15.0	0.946	1.730	-0.860	0.914	-2.863	-0.811
20.0	1.427	2.289	-0.985	0.539	-3.857	-1.121

MODEL CONFIGURATION: T17

YAW ANGLE	LIFT COEF.	DRAG COEF.	SIDE COEF.	PITCH COEF.	ROLL COEF.	YAW COEF.
-5.0	0.484	0.988	0.396	1.440	0.897	0.311
0.0	0.399	0.898	0.020	1.603	-0.065	0.029
5.0	0.501	0.994	-0.365	1.589	-1.063	-0.268
10.0	0.725	1.324	-0.751	1.428	-1.938	-0.555
15.0	0.984	1.825	-0.990	1.055	-2.812	-0.837
20.0	1.483	2.443	-1.196	0.748	-3.578	-1.143

MODEL CONFIGURATION: T18

YAW ANGLE	LIFT COEF.	DRAG COEF.	SIDE COEF.	PITCH COEF.	ROLL COEF.	YAW COEF.
-5.0	0.518	1.016	0.369	1.505	0.865	0.302
0.0	0.434	0.916	0.016	1.617	-0.113	0.026
5.0	0.542	1.022	-0.360	1.605	-1.086	-0.273
10.0	0.750	1.345	-0.671	1.470	-1.819	-0.494
15.0	0.971	1.837	-0.879	1.214	-2.462	-0.709
20.0	1.492	2.474	-1.079	1.044	-3.373	-1.022

MODEL CONFIGURATION: T19

YAW ANGLE	LIFT COEF.	DRAG COEF.	SIDE COEF.	PITCH COEF.	ROLL COEF.	YAW COEF.
-5.0	0.413	1.056	0.312	1.536	0.854	0.292
0.0	0.377	0.964	0.053	1.661	-0.088	0.048
5.0	0.461	1.060	-0.295	1.668	-1.025	-0.254
10.0	0.604	1.380	-0.462	1.602	-1.344	-0.321
15.0	0.826	1.848	-0.629	1.361	-1.750	-0.476
20.0	1.176	2.407	-0.768	1.140	-2.347	-0.716

MODEL CONFIGURATION: T20

YAW ANGLE	LIFT COEF.	DRAG COEF.	SIDE COEF.	PITCH COEF.	ROLL COEF.	YAW COEF.
-5.0	0.412	1.050	0.404	1.506	1.092	0.389
0.0	0.374	0.958	0.041	1.629	0.011	0.057
5.0	0.432	1.054	-0.344	1.613	-1.282	-0.328
10.0	0.578	1.383	-0.607	1.506	-1.650	-0.465
15.0	0.769	1.876	-0.797	1.206	-2.214	-0.653
20.0	1.007	2.488	-1.010	0.862	-3.049	-0.979

MODEL CONFIGURATION: T21

YAW ANGLE	LIFT COEF.	DRAG COEF.	SIDE COEF.	PITCH COEF.	ROLL COEF.	YAW COEF.
-5.0	0.317	1.007	-0.014	1.185	-0.523	-0.160
0.0	0.255	0.851	-0.098	1.077	-0.622	-0.144
5.0	0.310	0.975	-0.021	1.187	0.020	0.106
10.0	0.511	1.358	-0.147	1.424	-0.030	0.097
15.0	0.637	1.826	-0.362	1.292	-0.742	-0.146
20.0	0.901	2.332	-0.472	1.155	-1.390	-0.369

MODEL CONFIGURATION: T22

YAW ANGLE	LIFT COEF.	DRAG COEF.	SIDE COEF.	PITCH COEF.	ROLL COEF.	YAW COEF.
-5.0	0.306	1.019	-0.078	1.253	-0.709	-0.223
0.0	0.251	0.847	-0.124	1.074	-0.619	-0.166
5.0	0.302	0.994	0.047	1.236	0.372	0.208
10.0	0.472	1.350	-0.146	1.350	-0.086	0.081
15.0	0.597	1.835	-0.323	1.309	-0.631	-0.116
20.0	0.897	2.360	-0.455	1.307	-1.439	-0.375

MODEL CONFIGURATION: T23

YAW ANGLE	LIFT COEF.	DRAG COEF.	SIDE COEF.	PITCH COEF.	ROLL COEF.	YAW COEF.
-5.0	0.205	1.089	0.268	0.785	0.237	0.139
0.0	0.204	0.938	-0.007	0.829	-0.148	0.007
5.0	0.225	1.081	-0.278	0.805	-0.584	-0.154
10.0	0.369	1.465	-0.455	0.909	-0.833	-0.248
15.0	0.644	1.913	-0.486	0.931	-1.046	-0.323
20.0	1.032	2.432	-0.501	1.012	-1.412	-0.460

MODEL CONFIGURATION: T24

YAW ANGLE	LIFT COEF.	DRAG COEF.	SIDE COEF.	PITCH COEF.	ROLL COEF.	YAW COEF.
-5.0	0.218	1.088	0.271	0.763	0.268	0.150
0.0	0.213	0.937	-0.005	0.823	-0.095	0.015
5.0	0.242	1.080	-0.280	0.792	-0.659	-0.166
10.0	0.380	1.474	-0.454	0.905	-0.852	-0.249
15.0	0.643	1.914	-0.480	0.961	-1.107	-0.336
20.0	0.995	2.455	-0.502	1.060	-1.408	-0.453

MODEL CONFIGURATION: T25

YAW ANGLE	LIFT COEF.	DRAG COEF.	SIDE COEF.	PITCH COEF.	ROLL COEF.	YAW COEF.
-5.0	0.195	1.090	0.256	0.814	0.256	0.132
0.0	0.188	0.943	-0.011	0.850	-0.153	-0.003
5.0	0.213	1.086	-0.272	0.870	-0.560	-0.144
10.0	0.358	1.459	-0.450	0.934	-0.881	-0.256
15.0	0.660	1.906	-0.488	0.996	-1.059	-0.328
20.0	1.044	2.413	-0.472	1.054	-1.386	-0.438

MODEL CONFIGURATION: T26

YAW ANGLE	LIFT COEF.	DRAG COEF.	SIDE COEF.	PITCH COEF.	ROLL COEF.	YAW COEF.
-5.0	0.260	1.039	0.435	0.693	0.616	0.276
0.0	0.213	0.888	0.038	0.783	-0.046	0.041
5.0	0.277	1.034	-0.442	0.741	-0.963	-0.292
10.0	0.443	1.434	-0.804	0.713	-1.891	-0.604
15.0	0.677	1.926	-0.937	0.628	-2.329	-0.775
20.0	0.961	2.582	-1.170	0.445	-3.075	-1.074

MODEL CONFIGURATION: T27

YAW ANGLE	LIFT COEF.	DRAG COEF.	SIDE COEF.	PITCH COEF.	ROLL COEF.	YAW COEF.
-5.0	0.463	1.031	0.413	1.507	0.958	0.347
0.0	0.420	0.921	0.030	1.629	-0.031	0.042
5.0	0.508	1.030	-0.394	1.627	-1.154	-0.312
10.0	0.673	1.365	-0.697	1.546	-1.813	-0.513
15.0	0.909	1.875	-1.018	1.192	-2.780	-0.840
20.0	1.227	2.510	-1.264	0.761	-3.609	-1.167

MODEL CONFIGURATION: T28

YAW ANGLE	LIFT COEF.	DRAG COEF.	SIDE COEF.	PITCH COEF.	ROLL COEF.	YAW COEF.
-5.0	0.459	1.001	0.457	1.473	1.098	0.393
0.0	0.377	0.903	0.056	1.621	0.001	0.058
5.0	0.482	1.005	-0.413	1.607	-1.210	-0.321
10.0	0.649	1.336	-0.790	1.462	-2.043	-0.595
15.0	0.920	1.856	-1.143	1.013	-3.186	-0.983
20.0	1.257	2.496	-1.359	0.541	-3.978	-1.296

MODEL CONFIGURATION: T29

YAW ANGLE	LIFT COEF.	DRAG COEF.	SIDE COEF.	PITCH COEF.	ROLL COEF.	YAW COEF.
0.0	0.389	0.964	-0.027	1.654	0.200	0.018
0.0	0.379	0.966	-0.010	1.628	0.082	0.002
0.0	0.387	0.977	-0.001	1.676	0.073	0.010
0.0	0.392	0.972	0.005	1.683	0.052	0.014
0.0	0.393	0.976	0.009	1.683	0.044	0.015